

Iteris: Agentic Research Loops for Computational Mathematics

Leheng Chen^{1,5}, Zihao Liu^{1,5}, Wanyi He¹, Bin Dong^{2,3,4,5}[✉]

¹School of Mathematical Sciences, Peking University

²Beijing International Center for Mathematical Research and the New Cornerstone Science Laboratory, Peking University

³Center for Machine Learning Research, Peking University

⁴Center for Intelligent Computing, Great Bay Institute for Advanced Study, Great Bay University

⁵Zhongguancun Academy

Recent advances in large language models and agentic AI systems have enabled significant progress in mathematical discovery, from solving competition problems to tackling research-level conjectures. However, open problems in computational mathematics have received comparatively less attention: research in this area often requires not only proofs but also numerical experimentation, adversarial constructions, and algorithm design. In this paper, we introduce an agentic research system, Iteris, designed for open problems in computational mathematics. We apply Iteris to two open problems from a recent Simons Workshop collection [3]. In these case studies, Iteris generated numerical evidence, constructions, and proof drafts that led, after expert review and correction, to verified results. The first result is a phase diagram for the asymptotic comparison between conjugate gradient and randomized coordinate descent on power-law spectra; the second is a counterexample showing that QR factorization with column pivoting can fail to select well-conditioned submatrices even under low coherence. These case studies suggest that agentic AI systems can participate meaningfully in research workflows for open problems in computational mathematics, while human validation remains essential.

[✉]Corresponding author

✉ Correspondence : dongbin@math.pku.edu.cn

1 Introduction

Recent advances in large language models and agentic AI systems have opened new possibilities for mathematical discovery. Frontier reasoning models can now solve increasingly difficult competition and graduate-level problems through natural-language inference [7, 12, 24]. Beyond direct problem solving, systems such as FunSearch [22] and AlphaEvolve [20] have shown that language models can be embedded in iterative search loops, where candidate programs are generated, evaluated, and improved. More recently, autonomous mathematics systems have begun to target research-level questions, including long-horizon natural-language proof search, conjecture resolution, and human–AI co-mathematical workflows [10, 15, 26]. These developments suggest that AI systems are moving from solving isolated mathematical exercises toward participating in genuine mathematical research.

However, open problems in computational mathematics present a different kind of challenge. Progress in this area rarely consists of producing a proof in one pass, nor can it always be reduced to optimizing a single executable objective. A typical research trajectory may involve numerical experimentation, adversarial construction, and proof development. Thus computational mathematics requires an AI system to coordinate several research modes.

In this paper, we introduce Iteris, an agentic research system designed for open problems in computational mathematics. Iteris is organized as an explore–plan–execute loop. In each iteration, an exploration agent first probes plausible directions and tests whether the current branch is becoming locally stagnant. A plan agent then reads the global project state and chooses structured tasks for the next iteration. Specialized execution agents carry out the selected tasks, including foundation work, numerical experiment, proof construction,

and route review. All project state is maintained through files, which serve both as long-term memory and as structured messages between agents. This design allows Iteris to pursue long research trajectories while keeping research facts separate and checkable.

We apply Iteris to open problems from the recent collection *Linear Systems and Eigenvalue Problems: Open Questions from a Simons Workshop* [3]. Iteris produced long-horizon exploratory artifacts and proof drafts for these two problems; the final mathematical results were obtained after human verification, mathematical repair where needed, and expository reorganization. The first (*Problem 2.4*) concerns the asymptotic comparison between conjugate gradient (CG) and randomized coordinate descent (RCD) on power-law spectra. We establish a fixed-parameter phase diagram for the normalized cost ratio between RCD and CG; see Theorem 1. The second (*Problem 4.3*) concerns whether QR factorization with column pivoting (QRCP) reliably selects well-conditioned submatrices from a matrix with orthonormal row. We construct a low-coherence counterexample family showing that QRCP can fail to do so; see Theorem 2.

Iteris generated the main exploratory and deductive artifacts that made the two results possible, while the final mathematical arguments required expert verification and editing. In the CG case, the system found the main phase structure, but one rate analysis in the $p < 1$ regime initially relied on an unjustified stronger assumption; this gap was detected by human inspection and repaired through further human–AI interaction. In the QRCP case, the system identified the correct obstruction, but the generated proof trajectory was circuitous and required substantial reorganization into a readable proof.

Together, these results provide concrete evidence that agentic AI systems can move beyond benchmark problem solving and contribute to the research workflow for open problems in computational mathematics.

Contributions.

1. We describe the Iteris system: an explore–plan–execute agentic loop system for distinct research modes in computational mathematics.
2. We establish a fixed-parameter phase diagram for the CG-versus-RCD comparison on power-law spectra, giving asymptotic rates for the normalized cost ratio between RCD and CG (Theorem 1).
3. We answer the QRCP orthonormal-selection question in the negative by constructing a low-coherence orthonormal-row counterexample family (Theorem 2).

The rest of the paper is organized as follows. Section 2 reviews related work. Section 3 describes the Iteris system framework. Section 4 states the two open problems and their resolutions. Section 5 discusses broader implications. Appendices A and B give proof details.

2 Related work

AI systems for mathematical discovery. AI has increasingly become a tool for mathematical exploration and constructive search. Early work showed that machine learning can reveal patterns in mathematical data and help guide the formulation of new conjectures and theorems [8]. More recent systems use language models as search engines over explicit mathematical or algorithmic objects: FunSearch searches over programs with an automated evaluator [22], while AlphaEvolve extends evaluator-guided search to larger algorithmic code artifacts [20]. Research-level mathematics has also become an explicit target. First Proof proposed research-level mathematical questions as a benchmark for AI reasoning [1]; autonomous-mathematics systems such as Aletheia study long-horizon natural-language research processes [10]; and automated conjecture-resolution systems connect informal mathematical reasoning with formal verification [15]. Another important paradigm is human–AI collaboration: recent AI co-mathematician systems are designed to help pure mathematicians carry out research-level work through ideation, search, computation, and theorem proving [26]. These developments mark rapid progress in AI-assisted and increasingly autonomous mathematics, but open problems in applied and computational mathematics remain much less systematically explored.

Agentic research workflows. A parallel line of work views research automation as a long-horizon workflow rather than a single model call. ReAct introduced interleaved reasoning and acting in external environments [25],

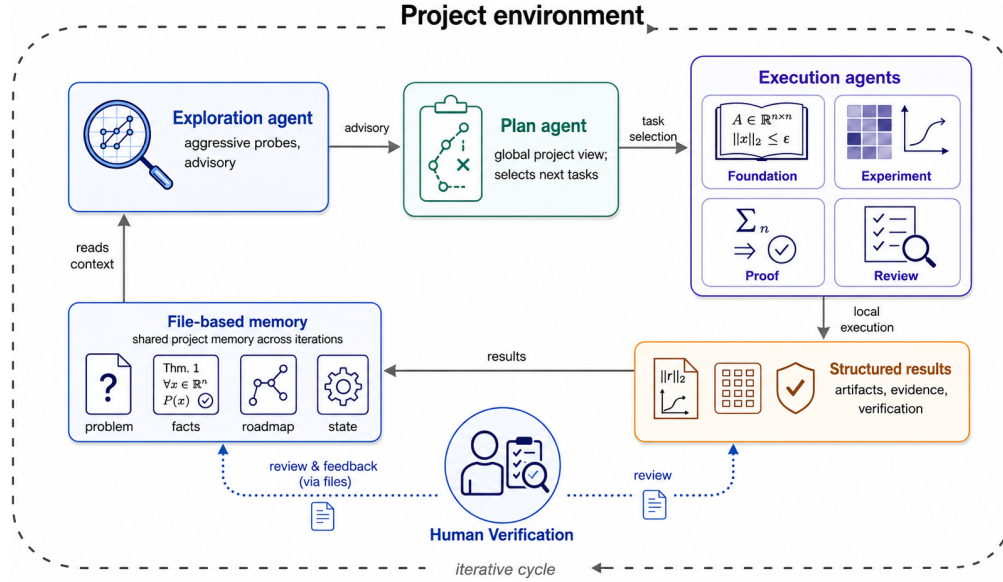


Figure 1 Iteris agent

and scientific agents such as Coscientist further demonstrate the use of LLM agents for scientific planning and experimentation [4]. Closest to full AI-research automation, The AI Scientist frames machine-learning research as an end-to-end agentic process spanning idea generation, literature search, experiment implementation, result analysis, manuscript drafting, and automated review [18]. These works establish agentic workflows as a promising route to scientific discovery, but they are mostly evaluated in laboratory, or benchmark-mediated settings; computational mathematics requires a tighter integration of numerical experimentation, algorithm design, and proof-sensitive reasoning.

3 Framework

Research in computational mathematics moves between several modes: formulating conjectures, running numerical tests, building proofs, and reviewing whether a route should continue. Iteris is an explore-plan-execute agentic loop system for coordinating these modes (Figure 1). The system has three main parts: an agentic explore-plan-execute protocol, execution agents for different research modes, and an exploration agent that tests possible directions before the plan agent chooses the next task pool.

3.1 Agentic explore-plan-execute protocol

Each iteration follows the same order: explore, plan, and execute. The three phases separate broad search, global task selection, and local research work:

1. Explore. **Exploration agent** runs probes before the next task pool is fixed. This work consists of light repository-level probing: reading relevant project files, inspecting recent iterations, searching prior facts, and drafting scratch reasoning over a few plausible routes. The exploration agent does not write the official plan. It writes scratch files and an advisory that records the recommended task shape, the local-minimum check, the routes considered, the reason the direction is high value now, and the risks or non-goals that keep the task safe.
2. Plan. **Plan agent** reads the project files and the exploration advisory. It has the global view of the project: the problem statement, roadmap, project memory, route status, prior facts, frontier state, and recent iteration results. Its job is to decide the task pool for the next iteration. The Plan agent writes `TASK_POOL.json`, which specifies each task’s category, goal, input files, allowed scope, verification requirements, and result contract.

3. **Execute.** Each selected **Execution agent** receives its assigned task from `TASK_POOL.json` as local context. It performs exactly one research action using its task-specific skills and writes structured result files. These result files are added back to project memory and become input for the next iteration.

The protocol is organized around files. Project files store memory across iterations, and they also pass structured information between agents. Thus files play two roles. First, they are memory: they keep the project state, reviewed facts, route decisions, and claim limits stable across many iterations. Second, they are messages: advisories, task pools, and result files move information from one agent to the next.

3.2 Execution agents for research modes

Execution agents implement the local research actions selected by the plan agent. Each execution agent is equipped with a task-specific agent skill: a Markdown-based capability specification that defines its purpose, admissible inputs, execution rules, and output schema. This makes different research modes reusable while keeping each execution step narrow and checkable.

Iteris currently uses four execution agent categories:

1. **Foundation agent:** audits sources, freezes definitions, drafts conjecture cards, and maintains claim discipline.
2. **Experiment agent:** runs numerical work, such as test harnesses, diagnostics, and counterexample searches. Experimental evidence is never treated as proof.
3. **Proof agent:** constructs and checks proof artifacts for stable statements, special cases, or route-level lemmas.
4. **Review agent:** evaluates evidence, proof gaps, route value, and claim status; it may recommend deepening, reframing, or retiring a branch.

The plan agent selects the execution agent categories needed in each iteration. This is similar to a mathematician deciding whether the next step should be source cleanup, computation, proof work, or strategic review. The selected execution agent does not make global project decisions. It applies the skills specified by `TASK_POOL.json` within the assigned scope and returns structured result files. This separation helps prevent false progress: numerical evidence, proof sketches, reviewed facts, and formal theorem claims are kept distinct.

3.3 Exploration agent for escaping local inertia

The exploration agent is separated from the plan agent because planning and exploration play different roles. This separation matters as the plan agent does not directly perform research actions. It works from the global project files, so it may keep improving the route that already looks most natural. This can be useful when the route is correct, but it can also lead to local parameter tuning or route inertia. In open problems, the useful next move may require trying a side idea before it is clear that the idea deserves an official task.

The exploration agent fills this gap by running aggressive probes. Its role is not to decide the official task pool, but to produce decision signals that help the plan agent avoid over-committing to the current branch. In practice, this means reviewing recent iterations, checking whether the branch has narrowed into incremental follow-up work, retrieving prior facts when they bear on the decision, and comparing a small number of plausible routes before recommending a candidate task shape. The plan agent may then adopt, modify, or reject this recommendation when writing `TASK_POOL.json`.

With this separation, planning remains globally coherent, execution remains locally scoped, and exploration gives the loop a way to search beyond its current path.

Together, these components form the Iteris system. In the open-problems section, we report two success-case trajectories in which Iteris ran for over a hundred iterations per problem and generated artifacts that contributed to the final results; the theorem statements and final proofs were verified, repaired where necessary, and organized by the authors. In our experiments, the generation agent is implemented using the OpenAI Codex agent with GPT-5.5 as the underlying model.

4 Open problems and resolutions

This section states the two mathematical problems from the Simons workshop collection [3]. For each problem we give the theorem statement, and a proof sketch. Full proof details appear in Appendices A and B. The proof of Problem II has also been verified in Lean¹.

4.1 Overview

Problem	Resolution type	Details
CG vs. RCD on power-law spectra	fixed-parameter phase diagram	Appendix A
QRCP orthonormal selection	counterexample	Appendix B

Table 1 The two open-problem resolutions reported in this paper.

4.2 Problem I: CG versus sketching

Background. Conjugate gradient (CG) [13, 23] and randomized sketch-and-project methods [11, 16, 19] are two classical iterative methods for solving symmetric positive-definite linear systems. They rely on different mechanisms: CG exploits global spectral structure through Krylov subspaces and residual polynomials, whereas randomized coordinate descent (RCD) and related coordinate sketch-and-project methods process only one coordinate at each step. The individual steps of RCD are therefore extremely cheap, but it may need more steps; the natural unit of comparison is an epoch, namely n coordinate updates, rather than a single coordinate step. The Simons workshop collection [3] *Problem 2.4* asks how these two mechanisms compare asymptotically in a source model with power-law spectra.

The problem concerns this epoch-scaled comparison in a regime where condition number alone is not predictive. The stopping times depend jointly on spectral decay, the source distribution of the right-hand side, and the orientation of the eigenvectors relative to the coordinate basis. Related work connects sketch-and-project convergence to randomized SVD [9] and analyzes subspace-constrained RCD [17]. We ask, for each fixed (p, ϵ) , which method has the asymptotic advantage and whether the answer forms a phase diagram.

Fix $p > 0$ and let

$$A_n = U_n \operatorname{diag}(1^{-p}, 2^{-p}, \dots, n^{-p}) U_n^*, \quad b_n = A_n z_n,$$

where $U_n \in \mathbb{C}^{n \times n}$ is Haar unitary and z_n is an independent uniformly distributed complex unit vector. Thus the exact solution is

$$x_{*,n} = A_n^{-1} b_n = z_n.$$

Both algorithms start from $x_0 = 0$, and errors are measured in the A_n -norm

$$\|v\|_{A_n}^2 = v^* A_n v.$$

The CG method is exact, unpreconditioned conjugate gradient. The randomized method is the coordinate sketch-and-project method used in the open problem: at step t , it samples $i_t \in \{1, \dots, n\}$ with probability

$$\mathbb{P}(i_t = i \mid A_n) = \frac{A_n(i, i)}{\operatorname{tr}(A_n)}$$

and performs the exact coordinate update

$$x_{t+1} = x_t + \frac{(b_n - A_n x_t)_{i_t}}{A_n(i_t, i_t)} e_{i_t}.$$

We write $I = (i_0, i_1, \dots)$ for the coordinate-sampling sequence.

¹<https://github.com/frenzymath/qr-cp-bounded-coherence-obstruction>

For a fixed relative squared-error threshold $\epsilon \in (0, 1)$, define

$$T_{\text{CG},n}(\epsilon, p) = \min \{t \geq 0 : \|x_t^{\text{CG}} - x_{\star,n}\|_{A_n}^2 \leq \epsilon \|x_0 - x_{\star,n}\|_{A_n}^2\},$$

and

$$T_{\text{RCD},n}(\epsilon, p; I) = \min \{t \geq 0 : \|x_t^{\text{RCD}}(I) - x_{\star,n}\|_{A_n}^2 \leq \epsilon \|x_0 - x_{\star,n}\|_{A_n}^2\}.$$

Since one RCD epoch consists of n coordinate updates, we compare CG steps with RCD epochs through

$$\rho_n(\epsilon, p) = \frac{T_{\text{RCD},n}(\epsilon, p; I)/n}{T_{\text{CG},n}(\epsilon, p)}.$$

The goal is to determine the fixed-parameter asymptotic behavior of $\rho_n(\epsilon, p)$ as $n \rightarrow \infty$.

Before stating the theorem, we introduce the CG-side quantity that will govern the phase diagram. It measures what fixed-degree residual polynomials can achieve in the power-law limit. For $0 < p < 1$, the limiting tail measure has only finitely many finite moments. Since a degree- k residual polynomial involves moments up to order $2k$, its limiting quadratic form is finite precisely when $(2k + 1)p < 1$.

Define

$$K(p) = \max\{k \geq 0 : (2k + 1)p < 1\},$$

and the limiting moment measure

$$\nu_p(dy) = \frac{1-p}{p} y^{-1/p} dy, \quad y \in [1, \infty).$$

We define the limiting CG floor by

$$F(p) = \min_{\deg r \leq K(p), r(0)=1} \int r(y)^2 \nu_p(dy).$$

This is a finite-dimensional moment problem. Equivalently, if

$$m_s(p) = \int y^s \nu_p(dy) = \frac{1-p}{1-(s+1)p}, \quad 0 \leq s \leq 2K(p),$$

and

$$G_{K(p)}(p) = (m_{a+b}(p))_{0 \leq a, b \leq K(p)},$$

then

$$F(p) = \frac{1}{(G_{K(p)}(p)^{-1})_{00}}.$$

Thus $F(p)$ is the constrained minimum of the finite Hankel moment matrix associated with ν_p .

Equivalently, if $G_K(p)_{ab} = \int y^{a+b} d\nu_p(y)$ on the active range, then

$$F(p) = \frac{1}{(G_{K(p)}(p)^{-1})_{00}}.$$

Intuitively, $F(p)$ is the lowest relative error level that fixed-degree CG can stably reach in the limiting active problem. The position of ϵ relative to $F(p)$ is the primary divider in the fixed-parameter phase diagram.

Theorem 1 (Fixed-parameter CG/RCD phase diagram with rate upper bounds). *Fix $p > 0$ and $\epsilon \in (0, 1)$. Then the zero-ratio regimes are:*

Regime	Conclusion	Proved upper bound
$p > 1$	$\rho_n(\epsilon, p) \xrightarrow{\mathbb{P}} 0$	$\rho_n(\epsilon, p) = O_{\mathbb{P}}(n^{-1})$
$p = 1$	$\rho_n(\epsilon, 1) \xrightarrow{\mathbb{P}} 0$	$\rho_n(\epsilon, 1) = O_{\mathbb{P}}\left(\frac{\log n}{a_n}\right)$
$1/3 < p < 1$	$F(p) = 1, \quad \rho_n(\epsilon, p) \xrightarrow{\mathbb{P}} 0$	$\rho_n(\epsilon, p) = O_{\mathbb{P}}(1/b_n)$
$p = 1/3$	$F(p) = 1, \quad \rho_n(\epsilon, 1/3) \xrightarrow{\mathbb{P}} 0$	$\rho_n(\epsilon, 1/3) = O_{\mathbb{P}}(1/b_n)$
$0 < p < 1/3, \epsilon < F(p)$	$\rho_n(\epsilon, p) \xrightarrow{\mathbb{P}} 0$	$\rho_n(\epsilon, p) = O_{\mathbb{P}}(1/b_n)$.

Here, in the $p = 1$ row the bound holds for every deterministic $a_n \rightarrow \infty$ satisfying

$$\log a_n = o(\log n),$$

whereas in the $O_{\mathbb{P}}(1/b_n)$ rows it holds for every deterministic $b_n \rightarrow \infty$ satisfying

$$b_n \log(1 + b_n) = o(\log n).$$

The remaining regimes are as follows.

(1) If $0 < p < 1/3$ and $F(p) < \epsilon < 1$, then there exists $\eta(p, \epsilon) > 0$ such that

$$\mathbb{P}(\rho_n(\epsilon, p) > \eta(p, \epsilon)) \rightarrow 1.$$

(2) If $0 < p < 1/3$ and $\epsilon = F(p)$, then there exist $\eta(p) > 0$ and $c(p) > 0$ such that

$$\liminf_{n \rightarrow \infty} \mathbb{P}(\rho_n(F(p), p) > \eta(p)) \geq c(p).$$

(3) Moreover, on the endpoint/lower-subband critical regimes

$$p = \frac{1}{2K+3} \quad \text{or} \quad \frac{1}{2K+3} < p \leq \frac{1}{2K+2}, \quad K \geq 1,$$

the critical obstruction strengthens to

$$\mathbb{P}(\rho_n(F(p), p) > \eta(p)) \rightarrow 1$$

for some $\eta(p) > 0$.

This theorem is pointwise in the fixed pair (p, ϵ) . The rate bounds are conservative stochastic upper bounds, included only to quantify the zero-ratio regimes. We do not claim that these bounds are sharp.

4.2.1 Proof sketch

First, we reduce exact CG to a finite-dimensional residual-polynomial minimum. Write

$$A_n = U_n \Lambda_n U_n^*, \quad \Lambda_n = \text{diag}(1^{-p}, 2^{-p}, \dots, n^{-p}), \quad \alpha = U_n^* z_n.$$

For $d \geq 0$, define

$$M_{d,n}(p) = \min_{\deg q \leq d, q(0)=1} \frac{\sum_{j=1}^n \lambda_j |q(\lambda_j)|^2 |\alpha_j|^2}{\sum_{j=1}^n \lambda_j |\alpha_j|^2}.$$

The standard CG optimality property gives

$$T_{\text{CG},n}(\epsilon, p) = \min\{d \geq 0 : M_{d,n}(p) \leq \epsilon\}.$$

Since z_n is uniform on the complex unit sphere, the spectral weights have the representation

$$(|\alpha_1|^2, \dots, |\alpha_n|^2) \stackrel{d}{=} \frac{(E_1, \dots, E_n)}{\sum_{i=1}^n E_i},$$

where E_1, \dots, E_n are independent mean-one exponential random variables. Thus CG stopping becomes a random weighted moment problem.

Second, for $0 < p < 1$, we identify the fixed-degree CG limit. Rescale the spectrum by

$$Y_{j,n} = \left(\frac{n}{j}\right)^p, \quad S_{a,n} = \sum_{j=1}^n Y_{j,n}^a E_j,$$

and define the random probability measure

$$\mu_n = \frac{1}{S_{1,n}} \sum_{j=1}^n Y_{j,n} E_j \delta_{Y_{j,n}}.$$

Then

$$M_{d,n}(p) = \min_{\deg r \leq d, r(0)=1} \int r(y)^2 \mu_n(dy).$$

For fixed degrees, the relevant moments of μ_n converge to those of

$$\nu_p(dy) = \frac{1-p}{p} y^{-1/p} dy, \quad y \in [1, \infty).$$

A degree- k residual polynomial requires moments up to order $2k$, and these moments are finite exactly when

$$(2k+1)p < 1.$$

This gives

$$K(p) = \max\{k \geq 0 : (2k+1)p < 1\},$$

and the limiting CG floor

$$F(p) = \min_{\deg r \leq K(p), r(0)=1} \int r(y)^2 \nu_p(dy).$$

The fixed-degree limit is

$$M_{d,n}(p) \xrightarrow{\mathbb{P}} F_{\min(d, K(p))}(p).$$

Third, this floor gives the main $0 < p < 1$ phase mechanism. If $\epsilon < F(p)$, then every fixed CG degree remains above the threshold with high probability, so

$$T_{\text{CG},n}(\epsilon, p) \rightarrow \infty \quad \text{in probability.}$$

At the same time, source RCD satisfies the epoch upper bound

$$T_{\text{RCD},n}(\epsilon, p; I)/n = O_{\mathbb{P}}(1).$$

Therefore

$$\rho_n(\epsilon, p) \rightarrow 0.$$

This includes the whole row $1/3 \leq p < 1$, because then $K(p) = 0$ and $F(p) = 1$.

If $0 < p < 1/3$ and $F(p) < \epsilon < 1$, the fixed-degree limit gives bounded CG stopping:

$$T_{\text{CG},n}(\epsilon, p) = O_{\mathbb{P}}(1).$$

On the other hand, a small-support argument shows that RCD still needs a positive fraction of an epoch. Hence the ratio is bounded away from zero with high probability.

Fourth, the remaining qualitative cases are handled separately. When $p > 1$, the spectrum is summable:

$$\sum_{j=1}^{\infty} j^{-p} < \infty.$$

The RCD process has a Hilbert-space random-projection limit, and a fixed number of RCD updates eventually reduces the source error below the threshold. Thus

$$T_{\text{RCD},n}(\epsilon, p; I) = O_{\mathbb{P}}(1),$$

and since $T_{\text{CG},n}(\epsilon, p) \geq 1$,

$$\rho_n(\epsilon, p) = O_{\mathbb{P}}(n^{-1}).$$

At the logarithmic boundary $p = 1$, RCD satisfies

$$T_{\text{RCD},n}(\epsilon, 1; I)/n = O_{\mathbb{P}}(\log n),$$

while the CG polynomial minimum remains above any fixed $\epsilon < 1$ for super-logarithmically growing degrees. This gives

$$\rho_n(\epsilon, 1) \rightarrow 0.$$

The critical boundary $\epsilon = F(p)$ is decided by the first inactive Schur-complement correction. In every nonvacuous active band, this correction gives a positive-probability obstruction to $\rho_n \rightarrow 0$. On the endpoint/lower-subband critical regimes, the same correction dominates with probability tending to one, giving the stronger high-probability obstruction.

Finally, the rate bounds use growing-degree CG non-stopping estimates. For $p = 1$, if

$$a_n \rightarrow \infty, \quad \log a_n = o(\log n),$$

then

$$\mathbb{P}(T_{\text{CG},n}(\epsilon, 1) \leq a_n) \rightarrow 0.$$

For the $0 < p < 1$ zero-ratio regimes, if

$$b_n \rightarrow \infty, \quad b_n \log(1 + b_n) = o(\log n),$$

then

$$\mathbb{P}(T_{\text{CG},n}(\epsilon, p) \leq b_n) \rightarrow 0.$$

The stochastic upper bounds follow from the event inclusion

$$\left\{ \rho_n(\epsilon, p) > \frac{B \text{budget}_n}{d_n} \right\} \subset \left\{ \frac{T_{\text{RCD},n}(\epsilon, p; I)}{n} > B \text{budget}_n \right\} \cup \{T_{\text{CG},n}(\epsilon, p) \leq d_n\}.$$

Here $\text{budget}_n = \log n$ and $d_n = a_n$ for $p = 1$, while $\text{budget}_n = 1$ and $d_n = b_n$ for $0 < p < 1$. This proves the rate bounds stated in the theorem.

Full details are given in Appendix A.

4.2.2 Trajectory analysis

Figure 2 summarizes the agent-collaboration trajectory that led from the original open problem to the final fixed-parameter phase diagram. The figure records the main mathematical roles played by different agents in the Iteris framework: source auditing and convention freezing, candidate proof generation, independent review, blocker identification, proof repair, and final human mathematical audit.

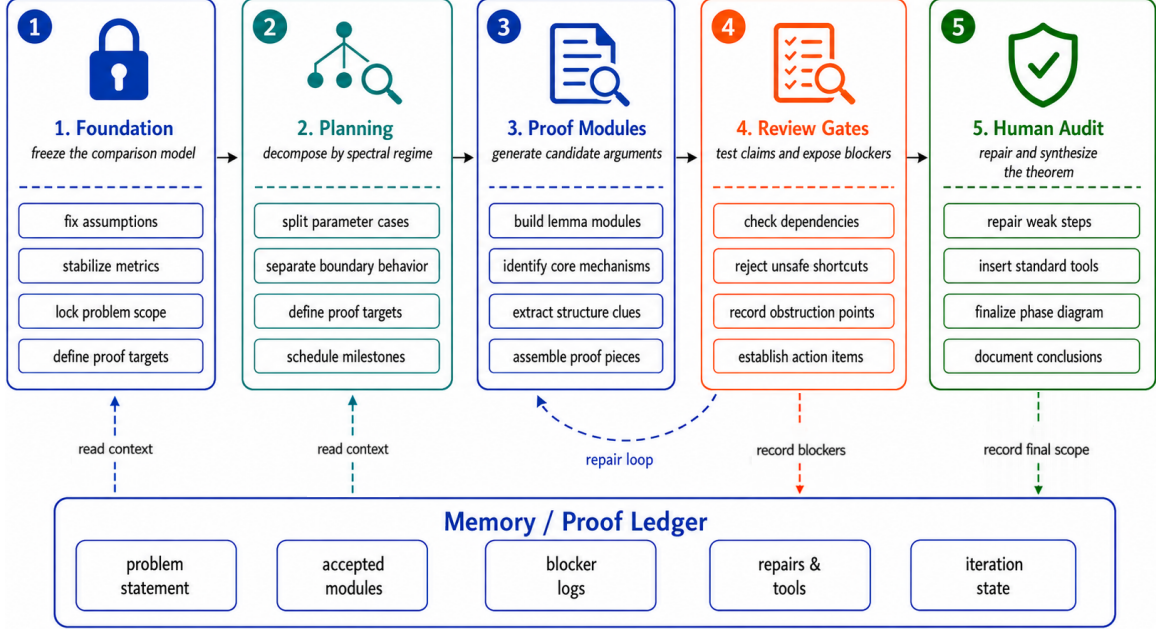


Figure 2 Iteris trajectory for Problem I.

1. *Foundation and model freeze.* The foundation stage fixed the exact comparison model from Problem 2.4 in the Simons workshop collection: Haar eigenvectors, power-law eigenvalues $\lambda_j = j^{-p}$, source right-hand side $b_n = A_n z_n$, exact unpreconditioned CG, and source RCD counted in epochs. This stage also fixed the comparison ratio $\rho_n(\varepsilon, p)$ and prevented later agents from silently changing the solver model, the source distribution, or the unit of comparison.

2. *Orchestrated decomposition.* The plan agent decomposed the original question into spectral regimes: the summable row $p > 1$, the logarithmic row $p = 1$, and the nonsummable range $0 < p < 1$. In the nonsummable range, it further separated the below-floor, above-floor, and critical-boundary cases. This orchestration turned the original open-ended comparison into smaller proof targets with explicit dependencies and review gates.

3. *Candidate proof generation.* Proof agents generated separate candidate modules for the CG polynomial representation, the RCD epoch upper bound, the RCD lower gate, the active moment problem, the $p = 1$ logarithmic row, the $p > 1$ summable row, and the critical Schur-complement boundary. These modules produced several positive mathematical outputs, including the identification of the active degree $K(p)$, the floor $F(p)$, the finite-dimensional residual-polynomial reduction, and the first-inactive Schur mechanism at the critical threshold.

4. *Review gates and blockers.* Review agents blocked several overstrong shortcuts: fixed-degree CG non-stopping was not allowed to imply growing-degree rate bounds; selected-row or proxy estimates were not automatically upgraded to global statements; and the critical boundary could not be justified by a compressed “standard asymptotics” step. These blockers forced the proof to split active-block estimates, Schur-gain estimates, inverse-coordinate stability, endpoint cases, and growing-degree controls into separate verifiable units.

5. *Repair loop and final audit.* The final appendix was produced only after these agent-generated modules were manually audited and repaired. In particular, informal or invalid arguments were replaced by standard mathematical tools: matrix Chernoff bounds for random Gram consistency, a projection-product theorem for the $p > 1$ Hilbert-space contraction, explicit Schur-complement asymptotics at the critical boundary, and a

separate treatment of the endpoint $K = 0$, i.e. $p = 1/3$. Thus the pipeline contributed both constructive proof modules and negative information about which proof routes were not justified.

The final proof in Appendix A should therefore be viewed as a human-audited synthesis of agent-generated and agent-reviewed proof modules. Two lessons from this trajectory are worth making explicit.

Direct GPT-Pro comparison. As a comparison point, we also submitted the same CG-versus-RCD question directly to GPT-Pro in an advanced reasoning mode.² The direct response produced an attractive heuristic picture: it identified reasonable spectral-filter intuition, proposed polynomial CG scalings, and suggested that epoch-scaled RCD should often dominate. However, it did not close the proof. In particular, it treated coordinate RCD too much like a diagonal spectral filter, blurred the distinction between expected, typical, and high-probability stopping times, and asserted sharp CG rates without the growing-degree lower bounds needed to justify them. This comparison clarifies one role of the Iteris framework: it does not merely ask for a more fluent answer, but decomposes a plausible heuristic into auditable proof obligations.

Human steering and rate-claim repair. A second lesson concerns the role of human steering. The initial agentic proof trajectory focused on the qualitative phase diagram. From a human mathematical perspective, however, such a qualitative convergence statement naturally calls for a more refined analysis of the speed of convergence. The model did not initially make this quantitative question explicit; only after human intervention did the proof search turn toward rate bounds.

Once this target was made explicit, early candidate proofs suggested a stronger negative-power rate for $\rho_n(\varepsilon, p)$. The subsequent review stage, again guided by the human request to check what was actually proved, identified that this rate claim was not supported by the available estimates. The fixed-degree CG argument showed only that $\mathbb{P}(T_{CG,n} \leq d) \rightarrow 0$ for every fixed d , whereas a negative-power bound for ρ_n would require a polynomial lower bound on $T_{CG,n}$. Subsequent discussion and repair replaced this overstrong statement by a conservative growing-degree non-stopping estimate. The final theorem therefore states bounds such as

$$\rho_n(\varepsilon, p) = O_{\mathbb{P}}(1/b_n), \quad b_n \rightarrow \infty, \quad b_n \log(1 + b_n) = o(\log n),$$

rather than an unsupported fixed negative exponent. This illustrates that the human intervention still matters: human mathematical judgment helped formulate the right rate question, while the agentic review and repair loop converted an overstrong candidate answer into a statement supported by the proof.

4.3 Problem II: QRCP orthonormal selection

Background. QR factorization with column pivoting (QRCP), introduced in the Householder least-squares setting by Businger and Golub [5], later became a standard deterministic tool for numerical rank detection, rank-revealing factorizations, and column-subset selection. Businger and Golub’s greedy pivot rule selects, at each step, the column with largest residual norm after projection. Subsequent theoretical work clarified the distinction between the existence of good rank-revealing column permutations and the behavior of particular pivoting rules. Hong and Pan [14] gave column permutation existence results for factorizations with provable singular-value bound, and Osinsky [21] gave a fairly efficient $O(nk^2)$ algorithm achieving this bound. The Simons workshop collection [3] *Problem 4.3* asks whether the classical QRCP enforces a conditioning guarantee in the orthonormal-row setting. Theorem 2 answers this question in the negative.

The problem concerns the rank-revealing power of exact QRCP in the orthonormal regime. Let $Q \in \mathbb{R}^{n \times k}$ have orthonormal columns, and apply QRCP to $A = Q^T$. Equivalently, at each step one selects the remaining row label whose column in A has largest squared residual after orthogonal projection away from the span already chosen. If $I_{\text{piv}} = (i_1, \dots, i_k)$ is the selected ordered set, write

$$M(Q) = Q[I_{\text{piv}}, :], \quad \gamma(Q, I_{\text{piv}}) = \|M(Q)^{-1}\|_2$$

²https://chatgpt.com/s/t_6a19b814f7508191822a0b542bb88347

when $M(Q)$ is nonsingular. The open question asks whether the residual-pivot rule forces $\gamma(Q, I_{\text{piv}})$ to stay under the scale $\sqrt{k(n-k+1)}$.

We prove a stronger obstruction: the residual-pivot rule can fail by an arbitrarily large polynomial factor even when the row energies of Q are uniformly controlled.

Theorem 2 (Bounded-coherence obstruction for QRCP). *For every $H_* > 1$, $B > 0$, $e \geq 0$, and $K \geq 1$, there exist integers $k \geq K$ and $n > k$, and a matrix $Q \in \mathbb{R}^{n \times k}$ with $Q^T Q = I_k$, such that QRCP applied to Q^T selects an ordered pivot set I_{piv} for which $M(Q)$ is nonsingular,*

$$\mu(Q) = \frac{n}{k} \max_{1 \leq i \leq n} \|Q(i, :)\|_2^2 < H_*, \quad \frac{\gamma(Q, I_{\text{piv}})}{\sqrt{k(n-k+1)}} > Bk^e.$$

Here $\mu(Q)$ is the standard coherence of the subspace $\text{range}(Q)$, i.e. the maximum row leverage score normalized by the average leverage k/n . The condition $\mu(Q) < H_*$ therefore places the example in a bounded-coherence regime. This rules out the explanation that the QRCP failure is caused by a few high-leverage rows. Such coherence conditions are ubiquitous in matrix completion and randomized linear algebra [6].

4.3.1 Proof sketch

We first prescribe the block that QRCP will select, make this block badly conditioned, and only afterwards add extra columns to restore orthonormality. Choose m large, set $k = m + 1$, and build

$$A \in \mathbb{R}^{k \times n}, \quad Q = A^T.$$

The columns of A are arranged in four blocks:

$$A = (R_+ \quad X \quad F \quad G).$$

The first block is the selected block

$$R_+ = \begin{pmatrix} R_\beta & z \\ 0 & \eta_p \end{pmatrix}.$$

Here R_β is an explicit upper-triangular chain. Let

$$\epsilon = e^{-\eta/k}, \quad s = (1 - \epsilon^2)^{1/2}, \quad d_t = \frac{1}{k} \epsilon^{t-1} \quad (1 \leq t \leq m),$$

and choose signs $\sigma_1, \dots, \sigma_m \in \{\pm 1\}$. Then

$$(R_\beta)_{t,q} = \begin{cases} d_t, & q = t, \\ -\frac{1}{2} \sigma_t \sigma_q s d_t, & t < q, \\ 0, & t > q. \end{cases}$$

The final selected column is $\begin{pmatrix} z \\ \eta_p \end{pmatrix}$, where

$$z_t = \frac{1}{4} \sigma_t s d_t \quad (t < m), \quad z_m = \frac{1}{4} \sigma_m \left(1 - \frac{1}{16}\right)^{1/2} d_m, \quad \eta_p = \frac{1}{4} d_m.$$

The signs are chosen so that the entries of $R_\beta^{-1} z$ reinforce rather than cancel. This triangular back-substitution is the source of the large inverse norm of the selected block.

The other three blocks only complete the identity $AA^T = I_k$, while keeping every added column too small to be selected by QRCP. The final selected column creates a mixed term between the first m coordinates and the last coordinate. We cancel this term by adding two cross columns

$$X = \begin{pmatrix} \theta_1 z & \theta_2 z \\ -b_1 \eta_p & -b_2 \eta_p \end{pmatrix}, \quad \theta_1 b_1 + \theta_2 b_2 = 1.$$

The mixed block from XX^T cancels exactly the mixed block from $R_+ R_+^T$.

After this cancellation, the remaining missing matrix in the first m coordinates is

$$M_{\text{rem}} = I_m - R_\beta R_\beta^T - (1 + \theta_1^2 + \theta_2^2) z z^T.$$

For large m this matrix is positive definite. We split it into many small rank-one pieces,

$$M_{\text{rem}} = \sum_{h=1}^{N_{\text{frame}}} W_h u_h u_h^T, \quad 0 < W_h < d_m^2, \quad \|u_h\|_2 = 1,$$

and put these pieces into the pure frame block

$$F = \begin{pmatrix} \sqrt{W_1} u_1 & \sqrt{W_2} u_2 & \cdots & \sqrt{W_{N_{\text{frame}}}} u_{N_{\text{frame}}} \\ 0 & 0 & \cdots & 0 \end{pmatrix}.$$

Thus F fills exactly the missing first-coordinate identity and contributes nothing to the last coordinate. The bound $W_h < d_m^2$ is also the pivot-control condition: before the final step, every frame column has residual below the next intended selected residual, and after the first m selected columns it has zero residual.

Only the last diagonal entry remains. We split the remaining scalar into positive pieces $e_1, \dots, e_{N_{\text{res}}}$ and set

$$G = \begin{pmatrix} 0 & 0 & \cdots & 0 \\ \sqrt{e_1} & \sqrt{e_2} & \cdots & \sqrt{e_{N_{\text{res}}}} \end{pmatrix}.$$

These residual-only columns complete the lower-right entry of AA^T .

Putting the blocks together, X cancels the mixed term, F restores the first-coordinate identity, and G restores the last diagonal entry. Hence

$$AA^T = I_k, \quad Q^T Q = I_k.$$

At the same time, the small-column bounds force QRCP to select the prescribed columns corresponding to R_+ , namely $I_{\text{piv}} = (1, 2, \dots, m, m+1)$.

It remains to quantify the bad conditioning of the selected block. Let $Z = \|R_\beta^{-1} z\|_2^2$.

Since

$$R_+ \begin{pmatrix} -R_\beta^{-1} z \\ 1 \end{pmatrix} = \begin{pmatrix} 0 \\ \eta_p \end{pmatrix},$$

the selected block has a very small singular direction, and therefore

$$\gamma(Q, I_{\text{piv}})^2 \geq \frac{Z}{\eta_p^2}.$$

The chosen sign pattern in the triangular chain makes Z grow exponentially which is faster than any fixed polynomial in k . The added columns increase the total row count, but only by the amount needed to complete the identity; this does not erase the growth coming from Z . Consequently, for sufficiently large k ,

$$\frac{\gamma(Q, I_{\text{piv}})}{\sqrt{k(n-k+1)}} > Bk^e.$$

Full details are given in Appendix B, where the coherence bound $\mu(Q) < H_*$ is also established. The proof has also been verified in Lean, with the aid of the autoformalization agent *Archon*³.

Both results were discovered and verified through the Iteris framework described in Section 3.

³<https://github.com/frenzymath/Archon>

4.3.2 Trajectory analysis

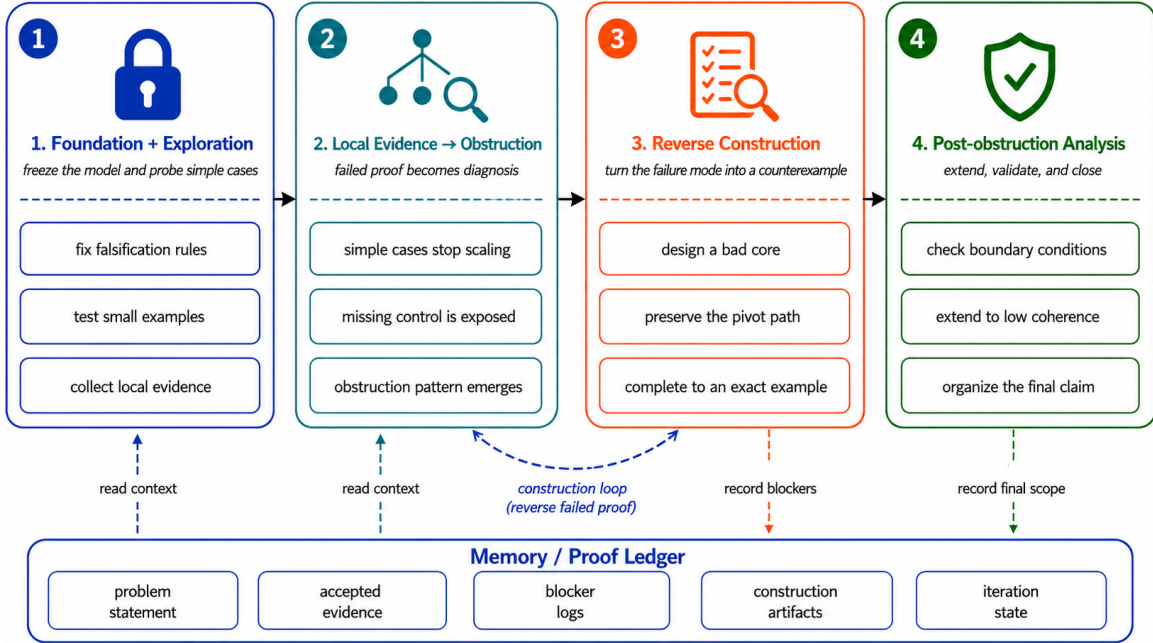


Figure 3 Iteris trajectory for Problem II.

In this problem, Iteris converts failed proof attempts into targeted structural obstruction insights to construct a exact counterexample and automatically extends to the low coherence setting.

1. *Model freeze and proof-oriented exploration.* Iteris first made the statement stable enough to prove or disprove: foundation agents fixed the QRCP convention, tie rule, quality measure, and falsification standard. With this target frozen, proof agents attacked simple cases ($k \leq 2$), experiment agents ran bounded searches and replays, and review agents kept the evidence scoped.

2. *From partial positive evidence to a localized obstruction.* The next phase was driven by the failure of these simple proof patterns to scale ($k \geq 3$). Small cases gave positive evidence, but the first genuinely nontrivial setting ($k = 3$) exposed a missing control: local residual norm and orthogonality do not by themselves control the cross interaction among the QRCP-selected rows. The failed proof attempt therefore became diagnostic. It identified the structure that a counterexample would need to exploit.

3. *Reversing the failed proof into an exact counterexample.* After this vulnerable structure was identified, the system shifted to reverse construction. It designed a selected core satisfying the local pivot conditions but violating the desired conditioning bound. Foundation work then turned the remaining issue into a completion problem: add unused rows to satisfy global orthogonality while preserving the intended QRCP pivot path. The counterexample thus came from reversing a failed proof structure, not from blind numerical search.

4. *Post-obstruction Analysis.* After identifying the obstruction, the system did not limit its analysis to this single case. The foundation and proof agents evaluated whether the mechanism could satisfy stricter regularity requirements. This process automatically extends the theorem to the low coherence construction of the obstruction.

The framework contribution is the controlled handoff between modes. File memory kept the statement, evidence, and route status stable. Foundation froze definitions and turned proof gaps into construction targets; experiment supplied diagnostics; proof exposed the obstruction; review controlled claim promotion and route

retirement. The QRCP case is therefore a trajectory from proof attempt, to obstruction insight and exact counterexample.

Direct GPT-Pro comparison. The direct response from GPT-Pro⁴ produced a meaningful high-level counterexample sketch. It correctly identified the relevant QRCP failure mechanism: a triangular block embedded through an orthogonal completion, can force the selected submatrix to be badly conditioned. The limitation was instead paper-quality closure. Several essential steps were treated as plausible rather than discharged as explicit, auditable obligations. The baseline also did not push the construction through boundary checks such as coherence and leverage constraints. Thus the comparison should not be read as GPT-Pro missing the main idea; rather, it clarifies one role of Iteris: turning a plausible counterexample mechanism into a closed, robust, and auditable construction.

Human audit and semantic alignment. The human role was primarily audit and organization. Iteris supplied the counterexample mechanism, intermediate construction artifacts, and boundary tests. Human work curated these outputs into a paper-level narrative and checked semantic consistency. After the formalization agent *Archon* completed Lean-level verification, the main human task was to align formal theorem statements and paper claims so that they referred to the same object and scope.

5 Discussion

Agentic research loops require reliable feedback, and computational mathematics is well suited because it offers both experimental and proof-based feedback. In both case studies, Iteris used numerical evidence to narrow candidate proof routes and mathematical proof to confirm or reject them. For instance, in the CG problem, numerical sweeps identified the Hankel floor as the key structural feature; in the QRCP construction, experiments isolated back-substitution pressure as the source-scale obstruction. Neither type of evidence alone was sufficient—numerical results guided search, and proofs settled claims.

The results produced by Iteris still required expert auditing to distinguish correct arguments from unsupported steps, and they required human reorganization to turn long and circuitous derivations into readable mathematical proofs. The two case studies illustrate different kinds of human intervention. In the CG case (Problem I), Iteris identified the main phase structure and generated much of the proof skeleton. However, one branch of the rate analysis in the $p < 1$ regime used a stronger assumption and led to an incorrect bound in that branch. Human inspection detected the mismatch, and the argument was repaired through subsequent human–AI interaction. In the QRCP case (Problem II), the construction and obstruction identified by Iteris were correct, but the proof was indirect and difficult to read. The final presentation therefore involved substantial human restructuring of the argument. The resulting construction has a sorry-free Lean 4 formalization of the core statement, but this does not eliminate the need to check that the formal statement matches the informal mathematical theorem.

Thus, Iteris shifts rather than removes human effort. In these case studies, the system was most valuable in broadening the search space, finding candidate structures, and producing draft arguments for human inspection. The human role remained essential for verifying assumptions, detecting gaps, repairing incorrect branches, and producing the final exposition. We therefore view Iteris as a tool for human-verified agentic research, not as a replacement for mathematical judgment.

Acknowledgements

The authors would like to warmly thank Zhangsong Li for carefully verifying the proof of CG-versus-sketching problem in Appendix A.

This work is supported in part by the Fundamental and Interdisciplinary Disciplines Breakthrough Plan of the Ministry of Education of China (JYB2025XDXM113), the National Key R&D Program of China grant 2024YFA1014000, and the New Cornerstone Investigator Program.

⁴https://chatgpt.com/s/t_6a1bf4501af8819191189ec9676c058e

References

- [1] Mohammed Abouzaid, Andrew J. Blumberg, Martin Hairer, Joe Kileel, Tamara G. Kolda, Paul D. Nelson, Daniel Spielman, Nikhil Srivastava, Rachel Ward, Shmuel Weinberger, and Lauren Williams. First proof, 2026. URL <https://arxiv.org/abs/2602.05192>.
- [2] Ichiro Amemiya and Tadao Ando. Convergence of random products of contractions in hilbert space. *Acta Scientiarum Mathematicarum*, 26(3–4):239–244, 1965.
- [3] Noah Amsel, Yves Baumann, Paul Beckman, Peter Bürgisser, Chris Camaño, Tyler Chen, Edmond Chow, Anil Damle, Michal Dereziński, Mark Embree, Ethan N. Epperly, Robert Falgout, Mark Fornace, Anne Greenbaum, Chen Greif, Diana Halikias, Zhen Huang, Elias Jarlebring, Yiannis Koutis, Daniel Kressner, Rasmus Kyng, Jörg Liesen, Jackie Lok, Raphael A. Meyer, Yuji Nakatsukasa, Kate Pearce, Richard Peng, David Persson, Eliza Rebrova, Ryan Schneider, Rikhav Shah, Edgar Solomonik, Nikhil Srivastava, Alex Townsend, Robert J. Webber, and Jess Williams. Linear systems and eigenvalue problems: Open questions from a simons workshop, 2026. URL <https://arxiv.org/abs/2602.05394>.
- [4] Daniil A. Boiko, Robert MacKnight, Ben Kline, and Gabe Gomes. Autonomous chemical research with large language models. *Nature*, 624(7992):570–578, December 2023. ISSN 1476-4687. doi: 10.1038/s41586-023-06792-0. URL <http://dx.doi.org/10.1038/s41586-023-06792-0>.
- [5] Peter Businger and Gene H. Golub. Linear least squares solutions by householder transformations. *Numerische Mathematik*, 7(3):269–276, 1965. ISSN 0945-3245. doi: 10.1007/bf01436084. URL <http://dx.doi.org/10.1007/bf01436084>.
- [6] Emmanuel J. Candès and Benjamin Recht. Exact matrix completion via convex optimization. *Foundations of Computational Mathematics*, 9(6):717–772, April 2009. ISSN 1615-3383. doi: 10.1007/s10208-009-9045-5. URL <http://dx.doi.org/10.1007/s10208-009-9045-5>.
- [7] Gheorghe Comanici, Eric Bieber, Mike Schaekermann, Ice Pasupat, Noveen Sachdeva, Inderjit Dhillon, Marcel Blistein, Ori Ram, Dan Zhang, Evan Rosen, et al. Gemini 2.5: Pushing the frontier with advanced reasoning, multimodality, long context, and next generation agentic capabilities. *arXiv preprint arXiv:2507.06261*, 2025.
- [8] Alex Davies, Petar Veličković, Lars Buesing, Sam Blackwell, Daniel Zheng, Nenad Tomašev, Richard Tanburn, Peter Battaglia, Charles Blundell, András Juhász, Marc Lackenby, Geordie Williamson, Demis Hassabis, and Pushmeet Kohli. Advancing mathematics by guiding human intuition with ai. *Nature*, 600(7887):70–74, December 2021. ISSN 1476-4687. doi: 10.1038/s41586-021-04086-x. URL <http://dx.doi.org/10.1038/s41586-021-04086-x>.
- [9] Michał Dereziński and Elizaveta Rebrova. Sharp analysis of sketch-and-project methods via a connection to randomized singular value decomposition. *SIAM Journal on Mathematics of Data Science*, 6(1):127–153, February 2024. ISSN 2577-0187. doi: 10.1137/23m1545537. URL <http://dx.doi.org/10.1137/23m1545537>.
- [10] Tony Feng, Trieu H. Trinh, Garrett Bingham, Dawsen Hwang, Yuri Chervovyi, Junehyuk Jung, Joonkyung Lee, Carlo Pagano, Sang hyun Kim, Federico Pasqualotto, Sergei Gukov, Jonathan N. Lee, Junsu Kim, Kaiying Hou, Golnaz Ghiasi, Yi Tay, YaGuang Li, Chenkai Kuang, Yuan Liu, Hanzhao Lin, Evan Zheran Liu, Nigamaa Nayakanti, Xiaomeng Yang, Heng-Tze Cheng, Demis Hassabis, Koray Kavukcuoglu, Quoc V. Le, and Thang Luong. Towards autonomous mathematics research, 2026. URL <https://arxiv.org/abs/2602.10177>.
- [11] Robert M. Gower and Peter Richtárik. Randomized iterative methods for linear systems. *SIAM Journal on Matrix Analysis and Applications*, 36(4):1660–1690, January 2015. ISSN 1095-7162. doi: 10.1137/15m1025487. URL <http://dx.doi.org/10.1137/15m1025487>.
- [12] Daya Guo, Dejian Yang, Haowei Zhang, Junxiao Song, Peiyi Wang, Qihao Zhu, Runxin Xu, Ruoyu Zhang, Shirong Ma, Xiao Bi, et al. Deepseek-r1 incentivizes reasoning in llms through reinforcement learning. *Nature*, 645(8081): 633–638, 2025.
- [13] M.R. Hestenes and E. Stiefel. Methods of conjugate gradients for solving linear systems. *Journal of Research of the National Bureau of Standards*, 49(6):409, December 1952. ISSN 0091-0635. doi: 10.6028/jres.049.044. URL <http://dx.doi.org/10.6028/jres.049.044>.
- [14] Y. P. Hong and C.-T. Pan. Rank-revealing qr factorizations and the singular value decomposition. *Mathematics of Computation*, 58(197):213, January 1992. ISSN 0025-5718. doi: 10.2307/2153029. URL <http://dx.doi.org/10.2307/2153029>.

- [15] Haocheng Ju, Guoxiong Gao, Jiedong Jiang, Bin Wu, Zeming Sun, Leheng Chen, Yutong Wang, Yuefeng Wang, Zichen Wang, Wanyi He, Peihao Wu, Liang Xiao, Ruochuan Liu, Bryan Dai, and Bin Dong. Automated conjecture resolution with formal verification, 2026. URL <https://arxiv.org/abs/2604.03789>.
- [16] D. Leventhal and A. S. Lewis. Randomized methods for linear constraints: Convergence rates and conditioning. *Mathematics of Operations Research*, 35(3):641–654, August 2010. ISSN 1526-5471. doi: 10.1287/moor.1100.0456. URL <http://dx.doi.org/10.1287/moor.1100.0456>.
- [17] Jackie Lok and Elizaveta Rebrova. Subspace-constrained randomized coordinate descent for linear systems with good low-rank matrix approximations, 2026. URL <https://arxiv.org/abs/2506.09394>.
- [18] Chris Lu, Cong Lu, Robert Tjarko Lange, Yutaro Yamada, Shengran Hu, Jakob Foerster, David Ha, and Jeff Clune. Towards end-to-end automation of ai research. *Nature*, 651(8107):914–919, March 2026. ISSN 1476-4687. doi: 10.1038/s41586-026-10265-5. URL <http://dx.doi.org/10.1038/s41586-026-10265-5>.
- [19] Yu. Nesterov. Efficiency of coordinate descent methods on huge-scale optimization problems. *SIAM Journal on Optimization*, 22(2):341–362, January 2012. ISSN 1095-7189. doi: 10.1137/100802001. URL <http://dx.doi.org/10.1137/100802001>.
- [20] Alexander Novikov, Ngãn Vũ, Marvin Eisenberger, Emilien Dupont, Po-Sen Huang, Adam Zsolt Wagner, Sergey Shirobokov, Borislav Kozlovskii, Francisco J. R. Ruiz, Abbas Mehrabian, M. Pawan Kumar, Abigail See, Swarat Chaudhuri, George Holland, Alex Davies, Sebastian Nowozin, Pushmeet Kohli, and Matej Balog. Alphaevolve: A coding agent for scientific and algorithmic discovery, 2025. URL <https://arxiv.org/abs/2506.13131>.
- [21] A.I. Osinsky. Close to optimal column approximation using a single svd. *Linear Algebra and its Applications*, 725:359–377, November 2025. ISSN 0024-3795. doi: 10.1016/j.laa.2025.07.016. URL <http://dx.doi.org/10.1016/j.laa.2025.07.016>.
- [22] Bernardino Romera-Paredes, Mohammadamin Barekatin, Alexander Novikov, Matej Balog, M. Pawan Kumar, Emilien Dupont, Francisco J. R. Ruiz, Jordan S. Ellenberg, Pengming Wang, Omar Fawzi, Pushmeet Kohli, and Alhussein Fawzi. Mathematical discoveries from program search with large language models. *Nature*, 625(7995): 468–475, December 2023. ISSN 1476-4687. doi: 10.1038/s41586-023-06924-6. URL <http://dx.doi.org/10.1038/s41586-023-06924-6>.
- [23] Yousef Saad. *Iterative Methods for Sparse Linear Systems*. Society for Industrial and Applied Mathematics, January 2003. ISBN 9780898718003. doi: 10.1137/1.9780898718003. URL <http://dx.doi.org/10.1137/1.9780898718003>.
- [24] An Yang, Anfeng Li, Baosong Yang, Beichen Zhang, Binyuan Hui, Bo Zheng, Bowen Yu, Chang Gao, Chengen Huang, Chenxu Lv, et al. Qwen3 technical report. *arXiv preprint arXiv:2505.09388*, 2025.
- [25] Shunyu Yao, Jeffrey Zhao, Dian Yu, Nan Du, Izhak Shafran, Karthik Narasimhan, and Yuan Cao. React: Synergizing reasoning and acting in language models, 2023. URL <https://arxiv.org/abs/2210.03629>.
- [26] Daniel Zheng, Ingrid von Glehn, Yori Zwols, Iuliya Beloshapka, Lars Buesing, Daniel M. Roy, Martin Wattenberg, Bogdan Georgiev, Tatiana Schmidt, Andrew Cowie, Fernanda Viegas, Dimitri Kanevsky, Vineet Kahlon, Hartmut Maennel, Sophia Alj, George Holland, Alex Davies, and Pushmeet Kohli. Ai co-mathematician: Accelerating mathematicians with agentic ai, 2026. URL <https://arxiv.org/abs/2605.06651>.

Appendix

A Proof details for CG versus sketching

This appendix proves Theorem 1. The proof is fixed-parameter throughout: p and ε are fixed before $n \rightarrow \infty$. The rate bounds proved below are conservative upper bounds; no matching lower bounds or sharpness claims are made.

A.1 Finite-dimensional reductions

Let

$$A_n = U_n \text{diag}(1^{-p}, \dots, n^{-p}) U_n^*, \quad b_n = A_n z_n, \quad x_{*,n} = z_n,$$

and let $\alpha = U_n^* z_n$. For $d \geq 0$, set

$$\mathcal{P}_d^1 = \{q \in \mathbb{R}[\xi] : \deg q \leq d, q(0) = 1\}$$

and

$$M_{d,n}(p) = \min_{q \in \mathcal{P}_d^1} \frac{\sum_{j=1}^n j^{-p} |q(j^{-p})|^2 |\alpha_j|^2}{\sum_{j=1}^n j^{-p} |\alpha_j|^2}.$$

Proposition 3 (CG polynomial representation). *Exact CG from $x_0 = 0$ satisfies*

$$T_{\text{CG},n}(\varepsilon, p) = \min\{d \geq 0 : M_{d,n}(p) \leq \varepsilon\}.$$

In particular $M_{0,n}(p) = 1$, so $T_{\text{CG},n}(\varepsilon, p) \geq 1$ for $\varepsilon \in (0, 1)$.

Proof. The d -th CG iterate minimizes the A_n -error over

$$\text{span}\{b_n, A_n b_n, \dots, A_n^{d-1} b_n\}.$$

Since $b_n = A_n z_n$, every vector in this space is $A_n s(A_n) z_n$ with $\deg s \leq d-1$. Hence the residual is

$$z_n - A_n s(A_n) z_n = q(A_n) z_n, \quad q(\xi) = 1 - \xi s(\xi),$$

where $q(0) = 1$ and $\deg q \leq d$. Conversely, every such q has this form because $1 - q(\xi)$ is divisible by ξ . Diagonalizing A_n gives exactly the displayed minimum. \square

The Haar vector satisfies

$$(|\alpha_1|^2, \dots, |\alpha_n|^2) \stackrel{d}{=} \frac{(E_1, \dots, E_n)}{\sum_i E_i}, \tag{A.1}$$

where the E_i are independent exponential variables of mean one. The common denominator cancels in $M_{d,n}$.

For $0 < p < 1$, define

$$Y_{j,n} = \left(\frac{n}{j}\right)^p, \quad S_{a,n} = \sum_{j=1}^n Y_{j,n}^a E_j, \quad \mu_n = \frac{1}{S_{1,n}} \sum_{j=1}^n Y_{j,n} E_j \delta_{Y_{j,n}}.$$

After the change of variables $r(y) = q(n^{-p}y)$,

$$M_{d,n}(p) = \min_{\deg r \leq d, r(0)=1} \int r(y)^2 \mu_n(dy). \tag{A.2}$$

Proposition 4 (RCD budget bounds). *Let $A \succ 0$ be deterministic, let $x_\star = A^{-1}b$, and run RCD from an arbitrary initial point x_0 . Write*

$$u_t = x_t - x_\star, \quad V_t = \|u_t\|_A^2,$$

and define

$$T_{\text{RCD}}(\varepsilon) = \min\{t \geq 0 : V_t \leq \varepsilon V_0\}.$$

At each step, RCD samples $i_t = i$ with probability

$$\mathbb{P}(i_t = i \mid A) = \frac{A(i, i)}{\text{tr}(A)}$$

and performs the exact coordinate update. Then, for every $k \geq 0$,

$$\mathbb{P}_I(T_{\text{RCD}}(\varepsilon) > k \mid A, u_0) \leq \varepsilon^{-1} \left(1 - \frac{\lambda_{\min}(A)}{\text{tr}(A)}\right)^k, \quad (\text{A.3})$$

where \mathbb{P}_I denotes probability over the RCD coordinate-sampling sequence only. Consequently, in the power-law model,

$$T_{\text{RCD},n}(\varepsilon, p; I)/n = O_{\mathbb{P}}(1), \quad 0 < p < 1, \quad (\text{A.4})$$

and

$$T_{\text{RCD},n}(\varepsilon, 1; I)/n = O_{\mathbb{P}}(\log n). \quad (\text{A.5})$$

Proof. Since $u_t = x_t - x_\star$, the exact coordinate update gives

$$u_{t+1} = u_t - \frac{(Au_t)_{i_t}}{A(i_t, i_t)} \mathbf{e}_{i_t},$$

where \mathbf{e}_i is the i -th coordinate vector. Therefore

$$V_{t+1} = V_t - \frac{|(Au_t)_{i_t}|^2}{A(i_t, i_t)}.$$

Taking expectation over i_t , conditionally on A and u_t , gives

$$\mathbb{E}_I[V_{t+1} \mid A, u_t] = V_t - \sum_i \frac{A(i, i)}{\text{tr}(A)} \frac{|(Au_t)_i|^2}{A(i, i)} = V_t - \frac{\|Au_t\|_2^2}{\text{tr}(A)}.$$

Since

$$\|Au_t\|_2^2 = u_t^* A^2 u_t \geq \lambda_{\min}(A) u_t^* A u_t = \lambda_{\min}(A) V_t,$$

we get

$$\mathbb{E}_I[V_{t+1} \mid A, u_t] \leq \left(1 - \frac{\lambda_{\min}(A)}{\text{tr}(A)}\right) V_t.$$

Iterating,

$$\mathbb{E}_I[V_k \mid A, u_0] \leq \left(1 - \frac{\lambda_{\min}(A)}{\text{tr}(A)}\right)^k V_0.$$

By Markov's inequality,

$$\mathbb{P}_I(T_{\text{RCD}}(\varepsilon) > k \mid A, u_0) = \mathbb{P}_I(V_k > \varepsilon V_0 \mid A, u_0) \leq \varepsilon^{-1} \left(1 - \frac{\lambda_{\min}(A)}{\text{tr}(A)}\right)^k.$$

For $A = A_n$, one has

$$\lambda_{\min}(A_n) = n^{-p}, \quad \text{tr}(A_n) = H_{n,p} := \sum_{j=1}^n j^{-p}.$$

If $0 < p < 1$, then

$$H_{n,p} \sim \frac{n^{1-p}}{1-p}, \quad \frac{n^{-p}}{H_{n,p}} = \frac{1-p}{n}(1+o(1)).$$

Taking $k = \lfloor Bn \rfloor$ gives an exponentially decaying upper tail in B , hence (A.4). If $p = 1$, then $H_{n,1} \sim \log n$. Taking $k = \lfloor Bn \log n \rfloor$ gives (A.5). \square

Proposition 5 (RCD lower gate). *Fix $0 < p < 1/3$ and $\varepsilon \in (0, 1)$. If $\gamma \in (0, 1)$ satisfies*

$$1 - \gamma^{1-p} > \varepsilon,$$

then there exists $a > 0$ such that

$$\mathbb{P}(T_{\text{RCD},n}(\varepsilon, p; I)/n > a) \rightarrow 1.$$

Proof. Let $a = \gamma/2$ and $k_n = \lfloor an \rfloor$. Write $I = (i_0, i_1, \dots)$ for the coordinate-sampling sequence, and define the selected-coordinate set

$$S_{k_n}(I) = \{i_0, \dots, i_{k_n-1}\}.$$

Since $x_0 = 0$ and each RCD step changes only one coordinate, the support of x_{k_n} is contained in $S_{k_n}(I)$. In particular,

$$|S_{k_n}(I)| \leq k_n \leq \gamma n.$$

For a deterministic coordinate set $S \subset \{1, \dots, n\}$, define

$$E_S = \text{span}\{\mathbf{e}_i : i \in S\},$$

where \mathbf{e}_i is the i -th coordinate vector. Let $P_{A_n, S}$ be the Euclidean orthogonal projection onto the subspace $A_n^{1/2}E_S$, and set

$$B_{A_n, S} = A_n^{1/2}(I - P_{A_n, S})A_n^{1/2}.$$

For every $x \in E_S$,

$$\|x - z_n\|_{A_n}^2 = \|A_n^{1/2}x - A_n^{1/2}z_n\|_2^2 \geq z_n^* B_{A_n, S} z_n.$$

Indeed, the right-hand side is the squared Euclidean distance from $A_n^{1/2}z_n$ to the subspace $A_n^{1/2}E_S$.

We next lower-bound $\text{tr}(B_{A_n, S})$. Since $P_{A_n, S}$ is an orthogonal projection of rank at most $|S|$, the Ky Fan maximum principle gives

$$\text{tr}(P_{A_n, S}A_n) \leq \sum_{j=1}^{|S|} j^{-p}.$$

Equivalently, this follows from the variational fact that among all rank- m orthogonal projections P , the maximum of $\text{tr}(PA_n)$ is the sum of the largest m eigenvalues of A_n . Therefore, if $|S| \leq \gamma n$,

$$\text{tr}(B_{A_n, S}) = \text{tr}(A_n) - \text{tr}(P_{A_n, S}A_n) \geq H_{n,p} - H_{\lfloor \gamma n \rfloor, p},$$

where $H_{m,p} = \sum_{j=1}^m j^{-p}$. Since

$$\frac{H_{\lfloor \gamma n \rfloor, p}}{H_{n,p}} \rightarrow \gamma^{1-p},$$

the assumption $1 - \gamma^{1-p} > \varepsilon$ implies that there exists $\theta > 0$ such that, for all sufficiently large n and all $|S| \leq \gamma n$,

$$\text{tr}(B_{A_n, S}) \geq (\varepsilon + \theta)H_{n,p}.$$

Now define

$$C_{A_n, S} = B_{A_n, S} - \varepsilon A_n.$$

Then

$$\mathrm{tr}(C_{A_n, S}) \geq \theta H_{n, p}.$$

Also $0 \leq B_{A_n, S} \leq A_n$, so

$$-\varepsilon A_n \leq C_{A_n, S} \leq (1 - \varepsilon) A_n.$$

Since $\|A_n\| = 1$, this gives

$$\|C_{A_n, S}\| \leq 1.$$

For a uniform complex unit vector z_n , the standard spherical quadratic form identities give, conditionally on A_n and S ,

$$\mathbb{E}[z_n^* C_{A_n, S} z_n \mid A_n, S] = \frac{\mathrm{tr}(C_{A_n, S})}{n} \geq c n^{-p}$$

for some $c > 0$, and

$$\mathrm{Var}(z_n^* C_{A_n, S} z_n \mid A_n, S) = \frac{\mathrm{tr}(C_{A_n, S}^2) - \mathrm{tr}(C_{A_n, S})^2/n}{n(n+1)} \leq \frac{1}{n}.$$

Chebyshev's inequality therefore yields, uniformly over all $|S| \leq \gamma n$,

$$\mathbb{P}(z_n^* C_{A_n, S} z_n \leq 0 \mid A_n, S) \leq C n^{2p-1} \rightarrow 0.$$

Here $p < 1/3$ is more than enough.

Finally, conditional on A_n and the coordinate-sampling sequence I , the set $S_{k_n}(I)$ is fixed and is independent of z_n . Since $|S_{k_n}(I)| \leq \gamma n$, the preceding bound applies with $S = S_{k_n}(I)$. Hence, with probability tending to one,

$$z_n^* B_{A_n, S_{k_n}(I)} z_n > \varepsilon z_n^* A_n z_n.$$

Because $x_{k_n} \in E_{S_{k_n}(I)}$, we have

$$V_{k_n} = \|x_{k_n} - z_n\|_{A_n}^2 \geq z_n^* B_{A_n, S_{k_n}(I)} z_n > \varepsilon z_n^* A_n z_n = \varepsilon V_0.$$

Thus $T_{\mathrm{RCD}, n}(\varepsilon, p; I) > k_n$ with probability tending to one. Since $k_n/n \rightarrow a$, the claim follows. \square

A.2 The active floor

For $0 < p < 1$, set

$$K(p) = \max\{k \geq 0 : (2k+1)p < 1\},$$

and

$$\nu_p(dy) = \frac{1-p}{p} y^{-1/p} dy, \quad y \in [1, \infty).$$

For $D \leq K(p)$, define

$$F_D(p) = \min_{\deg r \leq D, r(0)=1} \int r(y)^2 \nu_p(dy), \quad F(p) = F_{K(p)}(p).$$

Equivalently, if

$$m_s(p) = \int y^s \nu_p(dy) = \frac{1-p}{1-(s+1)p}, \quad 0 \leq s \leq 2D,$$

and

$$G_D(p) = (m_{a+b}(p))_{0 \leq a, b \leq D},$$

then $G_D(p)$ is positive definite. Indeed, for any nonzero coefficient vector $c = (c_0, \dots, c_D)$,

$$c^* G_D(p) c = \int \left| \sum_{a=0}^D c_a y^a \right|^2 \nu_p(dy) > 0,$$

because ν_p has infinite support on $[1, \infty)$. Hence $G_D(p)$ is invertible, and the constrained minimum is

$$F_D(p) = \frac{1}{(G_D(p)^{-1})_{00}}. \tag{A.6}$$

Lemma 6 (Moment convergence). *If $(m+1)p < 1$, then*

$$\int y^m \mu_n(dy) = \frac{S_{m+1,n}}{S_{1,n}} \xrightarrow{\mathbb{P}} \frac{1-p}{1-(m+1)p}. \quad (\text{A.7})$$

Moreover, on every fixed interval $[1, R]$, μ_n converges in moments to ν_p .

Proof. For $ap < 1$,

$$S_{a,n} = n^{ap} \sum_{j=1}^n j^{-ap} E_j, \quad \mathbb{E}S_{a,n} \sim \frac{n}{1-ap}, \quad \text{Var}(S_{a,n}) = o(n^2).$$

Hence $S_{a,n}/n \rightarrow (1-ap)^{-1}$ in probability. Taking $a = m+1$ and $a = 1$ proves (A.7). The local statement follows from the same law of large numbers on the index range $nR^{-1/p} \leq j \leq n$, followed by the change of variables $y = t^{-p}$. \square

Proposition 7 (Fixed-degree CG limit). *For fixed $0 < p < 1$ and fixed d ,*

$$M_{d,n}(p) \xrightarrow{\mathbb{P}} F_{\min(d, K(p))}(p). \quad (\text{A.8})$$

Proof. Let $D = \min(d, K(p))$. The upper bound follows by inserting the minimizer for $F_D(p)$ into (A.2) and using Lemma 6. For the lower bound, take a minimizer r_n in (A.2). Since $r \equiv 1$ is feasible, $\int r_n^2 d\mu_n \leq 1$. Moment convergence on $[1, 2]$ gives a positive definite local Gram limit, hence the coefficients of r_n are tight. Any coefficient limit r cannot have degree larger than $K(p)$: if $\deg r = \ell > K(p)$, then $(2\ell+1)p \geq 1$, so $\int_1^R r^2 d\nu_p \rightarrow \infty$, contradicting the bound $\int r_n^2 d\mu_n \leq 1$ after taking R fixed and large. Therefore every limit point has degree at most D , and local convergence followed by $R \rightarrow \infty$ gives the lower bound $F_D(p)$. \square

A.3 Qualitative phase diagram

Proposition 8 (Zero ratio below the floor). *If $0 < p < 1$ and $\varepsilon < F(p)$, then*

$$\rho_n(\varepsilon, p) \xrightarrow{\mathbb{P}} 0.$$

In particular, if $1/3 \leq p < 1$, then $K(p) = 0$, $F(p) = 1$, and the same conclusion holds for every $\varepsilon \in (0, 1)$.

Proof. For every fixed d , Proposition 7 gives

$$\mathbb{P}(T_{\text{CG},n}(\varepsilon, p) \leq d) = \mathbb{P}(M_{d,n}(p) \leq \varepsilon) \rightarrow 0.$$

Thus $T_{\text{CG},n} \rightarrow \infty$ in probability. By (A.4), $T_{\text{RCD},n}/n = O_{\mathbb{P}}(1)$. Hence

$$\mathbb{P}(\rho_n > \eta) \leq \mathbb{P}(T_{\text{RCD},n}/n > C) + \mathbb{P}(T_{\text{CG},n} \leq C/\eta),$$

and the conclusion follows by first taking $n \rightarrow \infty$, then $C \rightarrow \infty$. \square

Proposition 9 (Strictly above the floor). *If $0 < p < 1/3$ and $F(p) < \varepsilon < 1$, then there exists $\eta(p, \varepsilon) > 0$ such that*

$$\mathbb{P}(\rho_n(\varepsilon, p) > \eta(p, \varepsilon)) \rightarrow 1.$$

Proof. Take $d = K(p)$. By Proposition 7,

$$M_{d,n}(p) \rightarrow F(p) < \varepsilon$$

in probability, so $T_{\text{CG},n}(\varepsilon, p) \leq d$ with probability tending to one. Proposition 5 gives

$$T_{\text{RCD},n}(\varepsilon, p; I)/n > a$$

with probability tending to one for some $a > 0$. On the intersection, $\rho_n > a/d$. □

Lemma 10 (Random hyperplane contraction). *Let \mathcal{H} be a separable Hilbert space, and let G_0, G_1, \dots be iid nonzero random vectors whose law has full support in \mathcal{H} . For $g \neq 0$, let P_{g^\perp} be the orthogonal projection onto g^\perp . Then, for every fixed $h \in \mathcal{H}$,*

$$P_{G_{t-1}^\perp} \cdots P_{G_0^\perp} h \rightarrow 0 \quad \text{strongly almost surely.}$$

Proof. We use the projection-product theorem for random products of orthogonal projections in Hilbert space: for iid random closed subspaces M_t , the product $P_{M_{t-1}} \cdots P_{M_0}$ converges strongly almost surely to the orthogonal projection onto $\cap_{t \geq 0} M_t$ [2]. Applying this theorem with $M_t = G_t^\perp$ gives

$$P_{G_{t-1}^\perp} \cdots P_{G_0^\perp} h \rightarrow P_{\cap_{t \geq 0} G_t^\perp} h \quad \text{strongly almost surely.}$$

It remains only to identify the intersection. Since the law of G_0 has full support and \mathcal{H} is separable, every ball in a countable base has positive probability. By independence and Borel–Cantelli, each such ball is hit infinitely often by the sequence $\{G_t : t \geq 0\}$. Hence $\{G_t : t \geq 0\}$ is almost surely dense in \mathcal{H} , and therefore its closed linear span is all of \mathcal{H} . Thus

$$\bigcap_{t \geq 0} G_t^\perp = \{0\} \quad \text{almost surely.}$$

The projection-product limit is consequently $P_{\{0\}} h = 0$, which proves the claim. □

Lemma 11 (Summable-spectrum RCD contraction). *Fix $p > 1$. For every $\varepsilon, \delta \in (0, 1)$, there exists a finite integer $L = L(p, \varepsilon, \delta)$ such that*

$$\liminf_{n \rightarrow \infty} \mathbb{P}(T_{\text{RCD},n}(\varepsilon, p; I) \leq L) \geq 1 - \delta.$$

Proof. Let

$$\mathcal{H}_p = \left\{ v = (v_j)_{j \geq 1} : \|v\|_{\mathcal{H}_p}^2 := \sum_{j \geq 1} j^{-p} |v_j|^2 < \infty \right\}.$$

Since $p > 1$,

$$H_p := \sum_{j \geq 1} j^{-p} < \infty,$$

so a standard complex Gaussian sequence belongs to \mathcal{H}_p almost surely.

For $1 \leq i \leq n$, define the rescaled Haar row

$$g_{i,n} = \sqrt{n} U_n^* \mathbf{e}_i$$

and its weighted norm

$$D_{i,n} = \sum_{j=1}^n j^{-p} |g_{i,n,j}|^2.$$

Since

$$A_n(i, i) = \mathbf{e}_i^* U_n \Lambda_n U_n^* \mathbf{e}_i = \frac{1}{n} D_{i,n},$$

the RCD sampling probability is

$$\mathbb{P}(i_t = i \mid A_n) = \frac{A_n(i, i)}{\text{tr}(A_n)} = \frac{D_{i,n}}{nH_{n,p}}, \quad H_{n,p} = \sum_{j=1}^n j^{-p}.$$

The weighted empirical row law

$$\sum_{i=1}^n \frac{D_{i,n}}{nH_{n,p}} \delta_{g_{i,n}}$$

converges weakly, in probability, to the size-biased Gaussian law

$$Q(dg) = \frac{\|g\|_{\mathcal{H}_p}^2}{H_p} \Gamma(dg),$$

where Γ is the law of a standard complex Gaussian sequence in \mathcal{H}_p . The finite-coordinate marginals follow from the Gaussian representation of Haar rows, while the tail tightness follows from $\sum_{j \geq 1} j^{-p} < \infty$.

Now write the spectral error as

$$\beta_{t,n} = \sqrt{n} U_n^*(x_t - z_n).$$

For every fixed number of RCD steps, the process $(\beta_{t,n})$ converges to the Hilbert-space process

$$B_{t+1} = B_t - \frac{\langle G_t, B_t \rangle_{\mathcal{H}_p}}{\|G_t\|_{\mathcal{H}_p}^2} G_t, \quad G_t \stackrel{\text{iid}}{\sim} Q,$$

with $B_0 \sim \Gamma$. Equivalently,

$$B_{t+1} = P_{G_t^\perp} B_t.$$

The law Q has full support in \mathcal{H}_p . Therefore, by Lemma 10,

$$\|B_t\|_{\mathcal{H}_p} \rightarrow 0 \quad \text{almost surely.}$$

Equivalently,

$$\frac{\|B_t\|_{\mathcal{H}_p}^2}{\|B_0\|_{\mathcal{H}_p}^2} \rightarrow 0 \quad \text{almost surely.}$$

Thus, for the given ε, δ , one can choose a fixed integer L such that

$$\mathbb{P}\left(\|B_L\|_{\mathcal{H}_p}^2 \leq \varepsilon \|B_0\|_{\mathcal{H}_p}^2\right) \geq 1 - \delta.$$

The fixed-step convergence of $\beta_{t,n}$ to B_t then implies

$$\liminf_{n \rightarrow \infty} \mathbb{P}(T_{\text{RCD},n}(\varepsilon, p; I) \leq L) \geq 1 - \delta.$$

□

Proposition 12 (The summable row). *If $p > 1$, then*

$$T_{\text{RCD},n}(\varepsilon, p; I) = O_{\mathbb{P}}(1), \quad \rho_n(\varepsilon, p) = O_{\mathbb{P}}(n^{-1}).$$

Proof. By Lemma 11, for every $\delta > 0$ there exists a fixed $L < \infty$ such that

$$\liminf_{n \rightarrow \infty} \mathbb{P}(T_{\text{RCD},n}(\varepsilon, p; I) \leq L) \geq 1 - \delta.$$

This is exactly

$$T_{\text{RCD},n}(\varepsilon, p; I) = O_{\mathbb{P}}(1).$$

Since $T_{\text{CG},n}(\varepsilon, p) \geq 1$,

$$\rho_n(\varepsilon, p) = \frac{T_{\text{RCD},n}(\varepsilon, p; I)/n}{T_{\text{CG},n}(\varepsilon, p)} \leq \frac{T_{\text{RCD},n}(\varepsilon, p; I)}{n} = O_{\mathbb{P}}(n^{-1}).$$

□

A.4 The logarithmic row $p = 1$

Lemma 13 (Random Gram consistency under small leverage). *Let $a_{m,n} \in \mathbb{C}^r$ be deterministic vectors satisfying*

$$\sum_m a_{m,n} a_{m,n}^* = I_r, \quad \max_m \|a_{m,n}\|_2^2 \leq \tau_n.$$

Let E_m be independent mean-one exponential random variables. If

$$\tau_n \log r \rightarrow 0,$$

then

$$\left\| \sum_m (E_m - 1) a_{m,n} a_{m,n}^* \right\|_{\text{op}} \xrightarrow{\mathbb{P}} 0.$$

Proof. Set

$$X_n = \sum_m E_m a_{m,n} a_{m,n}^*.$$

Then

$$\mathbb{E} X_n = \sum_m a_{m,n} a_{m,n}^* = I_r.$$

The exponential matrix Chernoff bound for sums of independent positive semidefinite rank-one matrices gives the following estimate: for every fixed $0 < t < 1$, there is an absolute constant $c > 0$ such that

$$\mathbb{P}(\|X_n - I_r\|_{\text{op}} > t) \leq 2r \exp\left(-\frac{ct^2}{\tau_n}\right).$$

Since $\tau_n \log r \rightarrow 0$, the right-hand side tends to zero for every fixed $t > 0$. Therefore

$$\|X_n - I_r\|_{\text{op}} \xrightarrow{\mathbb{P}} 0.$$

Because

$$X_n - I_r = \sum_m (E_m - 1) a_{m,n} a_{m,n}^*,$$

the desired conclusion follows. \square

Proposition 14 (CG non-stopping at $p = 1$). *Let $a_n \rightarrow \infty$ be deterministic with*

$$\log a_n = o(\log n),$$

and set

$$d_n = \lfloor a_n \rfloor.$$

Then

$$M_{d_n, n}(1) \xrightarrow{\mathbb{P}} 1, \quad \mathbb{P}(T_{\text{CG}, n}(\varepsilon, 1) \leq a_n) \rightarrow 0.$$

Proof. Set

$$J_n = \lceil d_n^4 \rceil, \quad I_n = \{J_n, \dots, n\}.$$

Since $\log d_n = o(\log n)$, we have

$$\sum_{m \in I_n} \frac{1}{m} = \log n - \log J_n + O(1) = (1 - o(1)) \log n, \quad d_n^2 / J_n \rightarrow 0.$$

Consider the deterministic tail inner product

$$\langle f, g \rangle_n = \sum_{m \in I_n} \frac{f(1/m)g(1/m)}{m}.$$

We project the constant function -1 onto the span of the monomials

$$\xi, \xi^2, \dots, \xi^{d_n}.$$

The relevant Gram matrix and linear term are

$$G_{kl} = \sum_{m \in I_n} m^{-k-l-1}, \quad b_k = \sum_{m \in I_n} m^{-k-1}, \quad 1 \leq k, l \leq d_n.$$

Since $d_n^2/J_n \rightarrow 0$, these are asymptotic to a diagonally rescaled shifted Hilbert system:

$$G = R(H + o(1))R, \quad b = R(u + o(1)),$$

where

$$R = \text{diag}(J_n^{-1}, \dots, J_n^{-d_n}), \quad H_{kl} = \frac{1}{k+l}, \quad u_k = \frac{1}{k}.$$

The shifted Hilbert-matrix identity gives

$$u^\top H^{-1}u = 2 \sum_{\ell=1}^{d_n} \frac{1}{\ell} = O(\log d_n).$$

Therefore the projection energy is $O(\log d_n)$, and hence

$$\inf_{\deg q \leq d_n, q(0)=1} \sum_{m \in I_n} \frac{|q(1/m)|^2}{m} \geq \sum_{m \in I_n} \frac{1}{m} - O(\log d_n) = (1 - o(1)) \log n. \quad (\text{A.9})$$

It remains to pass from deterministic weights to exponential weights. Define

$$\tilde{v}_m = (1, m^{-1}, \dots, m^{-d_n})^\top, \quad \tilde{G} = \sum_{m \in I_n} m^{-1} \tilde{v}_m \tilde{v}_m^\top.$$

The Christoffel leverage bound in this tail window gives

$$\ell_m := m^{-1} \tilde{v}_m^\top \tilde{G}^{-1} \tilde{v}_m \leq C \frac{d_n^2}{J_n} = o(1).$$

Set

$$a_{m,n} = \tilde{G}^{-1/2} m^{-1/2} \tilde{v}_m.$$

Then

$$\sum_{m \in I_n} a_{m,n} a_{m,n}^\top = I_{d_n+1}, \quad \max_{m \in I_n} \|a_{m,n}\|_2^2 = o(1).$$

Since $d_n^2/J_n = d_n^{-2}(1 + o(1))$, the leverage bound satisfies the hypothesis of Lemma 13. Hence

$$\left\| \sum_{m \in I_n} (E_m - 1) \tilde{G}^{-1/2} m^{-1} \tilde{v}_m \tilde{v}_m^\top \tilde{G}^{-1/2} \right\|_{\text{op}} \xrightarrow{\mathbb{P}} 0.$$

Thus the random weighted quadratic form is relatively consistent with the deterministic one on the polynomial space, and (A.9) implies

$$\inf_{\deg q \leq d_n, q(0)=1} \sum_{m \in I_n} \frac{E_m |q(1/m)|^2}{m} \geq (1 - o_{\mathbb{P}}(1)) \log n.$$

Also,

$$\sum_{m=1}^n \frac{E_m}{m} = (1 + o_{\mathbb{P}}(1)) \log n.$$

Therefore

$$M_{d_n, n}(1) \geq 1 - o_{\mathbb{P}}(1).$$

The reverse inequality follows from the feasible polynomial $q \equiv 1$, so

$$M_{d_n, n}(1) \xrightarrow{\mathbb{P}} 1.$$

Since $\varepsilon < 1$,

$$\mathbb{P}(T_{\text{CG}, n}(\varepsilon, 1) \leq d_n) = \mathbb{P}(M_{d_n, n}(1) \leq \varepsilon) \rightarrow 0.$$

Finally, $T_{\text{CG}, n}$ is integer-valued and $d_n = \lfloor a_n \rfloor$, so

$$\{T_{\text{CG}, n}(\varepsilon, 1) \leq a_n\} = \{T_{\text{CG}, n}(\varepsilon, 1) \leq d_n\}.$$

This proves the proposition. \square

Proposition 15 (Rate at $p = 1$). *For every deterministic $a_n \rightarrow \infty$ satisfying*

$$\log a_n = o(\log n),$$

one has

$$\rho_n(\varepsilon, 1) = O_{\mathbb{P}}\left(\frac{\log n}{a_n}\right).$$

Proof. Use (A.5), Proposition 14, and the event inclusion

$$\left\{\rho_n > \frac{B \log n}{a_n}\right\} \subset \{T_{\text{RCD}, n}/n > B \log n\} \cup \{T_{\text{CG}, n} \leq a_n\}.$$

First take B large, then $n \rightarrow \infty$. \square

A.5 Critical boundary

At $\varepsilon = F(p)$, the active floor alone is not decisive. The proof uses the first inactive Schur-complement correction to the CG polynomial minimum.

Lemma 16 (Critical first-inactive Schur asymptotics). *The following first-inactive Schur asymptotics hold.*

(i) *If $K = 1$ and $1/5 < p < 1/3$, then*

$$F(p) = \frac{p^2}{(1-2p)^2}, \quad M_{1, n}(p) = 1 - \frac{S_{2, n}^2}{S_{1, n} S_{3, n}},$$

and

$$M_{2, n}(p) = M_{1, n}(p) - J_{2, n},$$

where

$$J_{2, n} = \frac{(S_{3, n}^2 - S_{2, n} S_{4, n})^2}{S_{1, n} S_{3, n} (S_{5, n} S_{3, n} - S_{4, n}^2)}.$$

Moreover,

$$M_{1, n}(p) - F(p) = O_{\mathbb{P}}(n^{3p-1}).$$

If $1/5 < p < 1/4$, then

$$n^{5p-1} J_{2, n} \Rightarrow L_{2, p}, \quad L_{2, p} > 0 \quad a.s.$$

If $p = 1/4$, then

$$n^{1/4}(\log n)^{-2}J_{2,n} \Rightarrow L_{2,1/4}, \quad L_{2,1/4} > 0 \quad a.s.$$

If $1/4 < p < 1/3$, then

$$n^{1-3p}(M_{1,n}(p) - F(p)) \Rightarrow c_p Z_p,$$

and

$$n^{1-3p}J_{2,n} \Rightarrow c_p \frac{\mathcal{A}_4^2}{\mathcal{A}_5},$$

where $c_p > 0$,

$$\mathcal{A}_4 = \sum_{j=1}^{\infty} j^{-4p} E_j, \quad \mathcal{A}_5 = \sum_{j=1}^{\infty} j^{-5p} E_j,$$

and

$$Z_p = \zeta_{\mathbb{R}}(3p) + \sum_{j=1}^{\infty} j^{-3p}(E_j - 1).$$

(ii) Fix $K \geq 2$ and

$$\frac{1}{2K+3} < p < \frac{1}{2K+1}.$$

Let $r_{K,n}$ be the degree- K minimizer for μ_n , and let $u_{K+1,n}$ be the component of y^{K+1} orthogonal to

$$\text{span}\{y, \dots, y^K\}$$

in $L^2(\mu_n)$. Then

$$M_{K+1,n}(p) = M_{K,n}(p) - J_{K+1,n}, \quad J_{K+1,n} = \frac{\ell_{K+1,n}^2}{s_{K+1,n}},$$

where

$$\ell_{K+1,n} = \int r_{K,n}(y) u_{K+1,n}(y) \mu_n(dy), \quad s_{K+1,n} = \int u_{K+1,n}(y)^2 \mu_n(dy).$$

The active-layer error satisfies

$$M_{K,n}(p) - F(p) = O_{\mathbb{P}}\left(n^{(2K+1)p-1}\right).$$

If

$$\frac{1}{2K+3} < p < \frac{1}{2K+2},$$

then

$$n^{(2K+3)p-1} J_{K+1,n} \Rightarrow L_{K,p}, \quad L_{K,p} > 0 \quad a.s.$$

If $p = 1/(2K+2)$, then

$$J_{K+1,n} = \frac{L_{K,p} + o_{\mathbb{P}}(1)}{\log n}, \quad L_{K,p} > 0.$$

(iii) If

$$\frac{1}{2K+2} < p < \frac{1}{2K+1}, \quad \alpha = 2K+1,$$

then

$$n^{1-\alpha p}(M_{K,n}(p) - F(p)) \Rightarrow C_{K,p} Z_{\alpha,p},$$

and

$$n^{1-\alpha p} J_{K+1,n} \Rightarrow C_{K,p} \frac{\mathcal{A}_{\alpha+1}^2}{\mathcal{A}_{\alpha+2}},$$

where $C_{K,p} > 0$,

$$\mathcal{A}_{\alpha+1} = \sum_{j=1}^{\infty} j^{-(\alpha+1)p} E_j, \quad \mathcal{A}_{\alpha+2} = \sum_{j=1}^{\infty} j^{-(\alpha+2)p} E_j,$$

and

$$Z_{\alpha,p} = \zeta_{\mathbb{R}}(\alpha p) + \sum_{j=1}^{\infty} j^{-\alpha p} (E_j - 1).$$

(iv) If $p_K = 1/(2K+3)$, $K \geq 1$, then

$$J_{K+1,n} = \frac{c_K}{\log n} (1 + o_{\mathbb{P}}(1)), \quad c_K > 0,$$

and

$$M_{K,n}(p_K) - F(p_K) = O_{\mathbb{P}}\left(n^{-2/(2K+3)}\right).$$

Proof. The proof is a direct Schur-complement expansion using the moment asymptotics of

$$S_{r,n} = \sum_{j=1}^n Y_{j,n}^r E_j.$$

The needed regimes are

$$S_{r,n} = \frac{n}{1-rp} (1 + o_{\mathbb{P}}(1)), \quad rp < 1,$$

$$S_{r,n} = n \log n (1 + o_{\mathbb{P}}(1)), \quad rp = 1,$$

and

$$n^{-rp} S_{r,n} \rightarrow \sum_{j=1}^{\infty} j^{-rp} E_j, \quad rp > 1.$$

In the upper subbands one also uses the Euler–Maclaurin fluctuation

$$n^{1-rp} \left(\frac{S_{r,n}}{n} - \frac{1}{1-rp} \right) \Rightarrow \zeta_{\mathbb{R}}(rp) + \sum_{j=1}^{\infty} j^{-rp} (E_j - 1),$$

valid in the L^2 -range $2rp > 1$.

For $K = 1$, the degree-one formula and the degree-two Schur complement give the displayed expression for $J_{2,n}$. Substituting the three moment regimes above yields the lower-subband, logarithmic, and upper-subband limits.

For $K \geq 2$, the degree- $(K+1)$ improvement is the Schur complement

$$J_{K+1,n} = \frac{\ell_{K+1,n}^2}{s_{K+1,n}}.$$

The numerator is determined by the coupling of the active minimizer with the first inactive direction y^{K+1} , while the denominator is the squared $L^2(\mu_n)$ -distance of y^{K+1} from the active span. Applying the same moment asymptotics gives the stated lower-subband, logarithmic, upper-subband, and endpoint estimates. The constants $L_{2,p}$, $L_{K,p}$, and c_K are strictly positive because the corresponding finite moment Gram Schur complements are strictly positive. \square

Proposition 17 (Critical boundary). *If $0 < p < 1/3$ and $\varepsilon = F(p)$, then there exist $\eta(p) > 0$ and $c(p) > 0$ such that*

$$\liminf_{n \rightarrow \infty} \mathbb{P}(\rho_n(F(p), p) > \eta(p)) \geq c(p).$$

Moreover, if

$$p = \frac{1}{2K+3} \quad \text{or} \quad \frac{1}{2K+3} < p \leq \frac{1}{2K+2}, \quad K \geq 1,$$

then the probability tends to one.

Proof. We first analyze the CG side and then combine it with the RCD lower gate.

Step 1: the band $K = 1$. Assume

$$\frac{1}{5} < p < \frac{1}{3}.$$

By Lemma 16,

$$M_{2,n}(p) = M_{1,n}(p) - J_{2,n}.$$

If $1/5 < p < 1/4$, then

$$M_{1,n}(p) - F(p) = O_{\mathbb{P}}(n^{3p-1}), \quad n^{5p-1} J_{2,n} \Rightarrow L_{2,p} > 0.$$

Since

$$1 - 5p > 3p - 1,$$

the Schur improvement dominates the active-layer error. Hence

$$\mathbb{P}(M_{2,n}(p) < F(p)) \rightarrow 1,$$

and therefore

$$\mathbb{P}(T_{\text{CG},n}(F(p), p) \leq 2) \rightarrow 1.$$

At $p = 1/4$, Lemma 16 gives

$$M_{1,n}(p) - F(p) = O_{\mathbb{P}}(n^{-1/4}),$$

and

$$n^{1/4}(\log n)^{-2} J_{2,n} \Rightarrow L_{2,1/4} > 0.$$

Thus $J_{2,n}$ again dominates the active error, and

$$\mathbb{P}(T_{\text{CG},n}(F(p), p) \leq 2) \rightarrow 1.$$

If $1/4 < p < 1/3$, Lemma 16 gives

$$n^{1-3p}(F(p) - M_{2,n}(p)) \Rightarrow c_p \left(\frac{\mathcal{A}_4^2}{\mathcal{A}_5} - Z_p \right).$$

The limiting random variable is positive with positive probability: indeed, $\mathcal{A}_4^2/\mathcal{A}_5 > 0$ almost surely, while

$$\mathbb{E}Z_p = \zeta_{\text{R}}(3p) < 0 \quad (0 < 3p < 1).$$

Hence

$$\liminf_{n \rightarrow \infty} \mathbb{P}(T_{\text{CG},n}(F(p), p) \leq 2) > 0.$$

Step 2: interior bands with $K \geq 2$. Fix $K \geq 2$ and assume

$$\frac{1}{2K+3} < p < \frac{1}{2K+1}.$$

By Lemma 16,

$$M_{K+1,n}(p) = M_{K,n}(p) - J_{K+1,n},$$

and

$$M_{K,n}(p) - F(p) = O_{\mathbb{P}}\left(n^{(2K+1)p-1}\right).$$

If

$$\frac{1}{2K+3} < p < \frac{1}{2K+2},$$

then

$$n^{(2K+3)p-1} J_{K+1,n} \Rightarrow L_{K,p} > 0.$$

Since

$$1 - (2K+3)p > (2K+1)p - 1,$$

the Schur improvement dominates the active-layer error. Hence

$$\mathbb{P}(T_{\text{CG},n}(F(p), p) \leq K+1) \rightarrow 1.$$

At

$$p = \frac{1}{2K+2},$$

Lemma 16 gives

$$J_{K+1,n} = \frac{L_{K,p} + o_{\mathbb{P}}(1)}{\log n}, \quad L_{K,p} > 0,$$

whereas

$$M_{K,n}(p) - F(p) = O_{\mathbb{P}}\left(n^{-1/(2K+2)}\right).$$

Again the Schur improvement dominates, so

$$\mathbb{P}(T_{\text{CG},n}(F(p), p) \leq K+1) \rightarrow 1.$$

If

$$\frac{1}{2K+2} < p < \frac{1}{2K+1},$$

let

$$\alpha = 2K+1.$$

Lemma 16 gives

$$n^{1-\alpha p}(F(p) - M_{K+1,n}(p)) \Rightarrow C_{K,p} \left(\frac{\mathcal{A}_{\alpha+1}^2}{\mathcal{A}_{\alpha+2}} - Z_{\alpha,p} \right).$$

The limiting variable is positive with positive probability because

$$\frac{\mathcal{A}_{\alpha+1}^2}{\mathcal{A}_{\alpha+2}} > 0 \quad \text{a.s.}, \quad \mathbb{E}Z_{\alpha,p} = \zeta_{\mathbb{R}}(\alpha p) < 0 \quad (0 < \alpha p < 1).$$

Thus

$$\liminf_{n \rightarrow \infty} \mathbb{P}(T_{\text{CG},n}(F(p), p) \leq K+1) > 0.$$

Step 3: odd-reciprocal endpoints. Let

$$p_K = \frac{1}{2K+3}, \quad K \geq 1.$$

By Lemma 16,

$$J_{K+1,n} = \frac{c_K}{\log n}(1 + o_{\mathbb{P}}(1)), \quad c_K > 0,$$

and

$$M_{K,n}(p_K) - F(p_K) = O_{\mathbb{P}}\left(n^{-2/(2K+3)}\right).$$

Since $1/\log n$ dominates $n^{-2/(2K+3)}$,

$$\mathbb{P}(T_{\text{CG},n}(F(p_K), p_K) \leq K + 1) \rightarrow 1.$$

Step 4: combination with the RCD lower gate. For $0 < p < 1/3$, one has $F(p) < 1$. Hence Proposition 5 applies at $\varepsilon = F(p)$: there exists $a(p) > 0$ such that

$$\mathbb{P}(T_{\text{RCD},n}(F(p), p; I)/n > a(p)) \rightarrow 1.$$

If the CG stopping event has positive liminf probability, then on the intersection

$$\rho_n(F(p), p) \geq \frac{a(p)}{K(p) + 1}.$$

This gives constants $\eta(p) > 0$ and $c(p) > 0$ such that

$$\liminf_{n \rightarrow \infty} \mathbb{P}(\rho_n(F(p), p) > \eta(p)) \geq c(p).$$

On the endpoint/lower-subband regimes, the CG stopping event has probability tending to one, so the same argument gives

$$\mathbb{P}(\rho_n(F(p), p) > \eta(p)) \rightarrow 1$$

for some $\eta(p) > 0$. □

A.6 Growing-degree rate bounds for $0 < p < 1$

The zero-ratio rows with $0 < p < 1$ use a conservative growing-degree non-stopping estimate. Throughout this subsection,

$$\langle f, g \rangle_n = \int f(y)g(y) \mu_n(dy), \quad \|f\|_n^2 = \langle f, f \rangle_n.$$

Let $K = K(p)$. Let $r_{K,n}$ be the degree- K minimizer in $L^2(\mu_n)$ subject to $r(0) = 1$. Thus

$$M_{K,n}(p) = \|r_{K,n}\|_n^2.$$

If $K \geq 1$, then

$$\langle r_{K,n}, y^a \rangle_n = 0, \quad 1 \leq a \leq K,$$

and we set

$$V_{K,n} = \text{span}\{y, \dots, y^K\}.$$

If $K = 0$, then

$$r_{0,n} \equiv 1, \quad V_{0,n} = \{0\}.$$

Lemma 18 (Growing-degree Schur bound). *Let $d = d_n \rightarrow \infty$ be deterministic and satisfy*

$$d \log(1 + d) = o(\log n).$$

Then

$$M_{K,n}(p) - M_{d,n}(p) = o_{\mathbb{P}}(1).$$

More precisely:

(i) *If p is not an odd reciprocal endpoint, then there are constants $A, C < \infty$ and $\beta = \beta(p) > 0$ such that*

$$0 \leq M_{K,n}(p) - M_{d,n}(p) \leq O_{\mathbb{P}}\left(e^{Cd \log(1+d)} d^A (\log n)^A n^{-\beta}\right). \quad (\text{A.10})$$

(ii) If $p = p_K = 1/(2K + 3)$, then there are constants $A, C, c > 0$ such that

$$0 \leq M_{K,n}(p_K) - M_{d,n}(p_K) \leq O_{\mathbb{P}}\left(\frac{1}{\log n - Cd \log(1+d)}\right) + O_{\mathbb{P}}\left(e^{Cd \log(1+d)} d^A (\log n)^A n^{-c}\right). \quad (\text{A.11})$$

Proof. The Schur-complement form of the improvement from degree K to degree d is

$$M_{K,n} - M_{d,n} = \sup_{0 \neq s \in \text{span}\{y, \dots, y^d\}} \frac{\langle r_{K,n}, s \rangle_n^2}{\|s\|_n^2}. \quad (\text{A.12})$$

Write

$$s(y) = \sum_{k=1}^d c_k y^k, \quad a_k = n^{pk} c_k.$$

At the first d spectral nodes $Y_{j,n} = (n/j)^p$,

$$s(Y_{j,n}) = \sum_{k=1}^d a_k j^{-pk}.$$

The Vandermonde matrix $B_d = (j^{-pk})_{1 \leq j, k \leq d}$ satisfies

$$\|B_d^{-1}\| \leq \exp\{Cd \log(1+d)\}.$$

Indeed, the node separation

$$|i^{-p} - j^{-p}| \geq c_p d^{-p-1} |i - j|$$

and the Lagrange interpolation formula give this inverse bound. Since $\min_{1 \leq j \leq d} E_j \geq d^{-3}$ with probability tending to one and $S_{1,n}/n = O_{\mathbb{P}}(1)$ with inverse tight, we get

$$\|s\|_n^2 \geq n^{p-1} e^{-Cd \log(1+d)} \sum_{k=1}^d a_k^2 \quad (\text{A.13})$$

with high probability.

For the numerator, the orthogonality of $r_{K,n}$ to y, \dots, y^K gives

$$\langle r_{K,n}, s \rangle_n = \sum_{k=K+1}^d a_k \gamma_{k,n}, \quad \gamma_{k,n} = n^{-pk} \langle r_{K,n}, y^k \rangle_n.$$

The coefficients of $r_{K,n}$ are tight, and for $0 \leq a \leq K$, $K+1 \leq k \leq d$,

$$\langle y^a, y^k \rangle_n = \frac{S_{a+k+1,n}}{S_{1,n}}.$$

A union bound over $k \leq d$, together with Markov estimates for these moments, gives

$$\sum_{k=K+1}^d \gamma_{k,n}^2 = O_{\mathbb{P}}\left(d^A (\log n)^A [n^{-2p(K+1)} + n^{2(K+1)p-2}]\right). \quad (\text{A.14})$$

Combining (A.12), (A.13), and (A.14),

$$M_{K,n} - M_{d,n} \leq O_{\mathbb{P}}\left(e^{Cd \log(1+d)} d^A (\log n)^A [n^{1-(2K+3)p} + n^{(2K+1)p-1}]\right).$$

If p is not an odd reciprocal endpoint, then

$$(2K + 1)p < 1 < (2K + 3)p,$$

so the bracket is $O(n^{-\beta})$ for some $\beta(p) > 0$. This proves (A.10).

It remains to explain the endpoint $p = p_K = 1/(2K + 3)$. The first inactive direction y^{K+1} is logarithmic and has to be separated from the higher inactive block. Using the convention above, define

$$u_n = (I - P_{V_{K,n}})y^{K+1},$$

and

$$B_{d,n} = (I - P_{V_{K,n}}) \text{span}\{y^{K+2}, \dots, y^d\},$$

where projections are in $L^2(\mu_n)$. Since $r_{K,n} \perp V_{K,n}$,

$$M_{K,n} - M_{d,n} = \|P_{\text{span}\{u_n\} + B_{d,n}} r_{K,n}\|_n^2.$$

A deterministic two-subspace projection estimate gives

$$\|P_{\text{span}\{u_n\} + B_{d,n}} r_{K,n}\|_n^2 \leq O_{\mathbb{P}}(1) \left(\|P_{B_{d,n}} r_{K,n}\|_n^2 + \frac{|\langle r_{K,n}, u_n \rangle_n|^2}{\text{dist}_n^2(u_n, B_{d,n})} \right). \quad (\text{A.15})$$

At the endpoint, the distance term is logarithmic:

$$\text{dist}_n^2(u_n, B_{d,n}) \geq c(\log n - Cd \log(1 + d))$$

with high probability. This is the endpoint Christoffel estimate obtained by changing variables $t = \log y$: the problem becomes the projection of a constant on an interval of length $p \log n$ against an exponential system, whose Cauchy Gram matrix loses only $O(d \log(1 + d))$. The random version follows from the same small-leverage Gram consistency used in the $p = 1$ row.

Moreover,

$$\langle r_{K,n}, u_n \rangle_n = \langle r_{K,n}, y^{K+1} \rangle_n = O_{\mathbb{P}}(1),$$

because the highest active moment involved is still subcritical. Thus the first inactive direction contributes the first term in (A.11). The block $B_{d,n}$ is controlled by the same Vandermonde argument as above, now starting at $K + 2$, which gives the second term in (A.11). Since $d \log(1 + d) = o(\log n)$, both terms are $o_{\mathbb{P}}(1)$. \square

Proposition 19 (Growing-degree CG non-stopping). *Assume $0 < p < 1$, $\varepsilon < F(p)$, and let $b_n \rightarrow \infty$ satisfy*

$$b_n \log(1 + b_n) = o(\log n). \quad (\text{A.16})$$

Then

$$\mathbb{P}(T_{\text{CG},n}(\varepsilon, p) \leq b_n) \rightarrow 0.$$

Proof. Set

$$d_n = \lfloor b_n \rfloor.$$

Then $d_n \rightarrow \infty$, $d_n \log(1 + d_n) = o(\log n)$, and since $T_{\text{CG},n}$ is integer-valued,

$$\{T_{\text{CG},n}(\varepsilon, p) \leq b_n\} = \{T_{\text{CG},n}(\varepsilon, p) \leq d_n\}.$$

By Proposition 7,

$$M_{K,n}(p) \xrightarrow{\mathbb{P}} F(p).$$

By Lemma 18,

$$0 \leq M_{K,n}(p) - M_{d_n,n}(p) = o_{\mathbb{P}}(1).$$

Hence

$$M_{d_n, n}(p) \geq F(p) - o_{\mathbb{P}}(1).$$

Choose $\delta = (F(p) - \varepsilon)/2 > 0$. Then

$$\mathbb{P}(M_{d_n, n}(p) \leq \varepsilon) \leq \mathbb{P}(M_{d_n, n}(p) < F(p) - \delta) \rightarrow 0.$$

Using the CG polynomial representation,

$$\mathbb{P}(T_{\text{CG}, n}(\varepsilon, p) \leq b_n) \rightarrow 0.$$

□

Proposition 20 (Rate for $0 < p < 1$). *In every zero-ratio row with $0 < p < 1$, if $b_n \rightarrow \infty$ and*

$$b_n \log(1 + b_n) = o(\log n),$$

then

$$\rho_n(\varepsilon, p) = O_{\mathbb{P}}(1/b_n).$$

Proof. Use (A.4), Proposition 19, and

$$\left\{ \rho_n > \frac{B}{b_n} \right\} \subset \{T_{\text{RCD}, n}/n > B\} \cup \{T_{\text{CG}, n} \leq b_n\}.$$

First choose B large, then let $n \rightarrow \infty$.

□

A.7 Completion

The zero-ratio rows are Proposition 12, Proposition 15, Proposition 8, and Proposition 20. The strictly above-floor positive-ratio row is Proposition 9. The critical boundary is Proposition 17.

All statements are fixed-parameter statements. The displayed rates are proved conservative upper bounds, not sharp rates. The proof does not address matching lower bounds, uniformity in p or K , moving thresholds, finite-precision effects, preconditioning, restarted CG, non-Haar eigenvectors, alternative sketching rules, or solver-level performance comparisons.

B Proof details for the QRCP obstruction

This appendix records the proof structure behind Theorem 2. The purpose is to make the counterexample readable as a mathematical construction rather than as a computational search log.

The proof is organized as follows. We first state the construction. We then prove five named estimates: pivot order, Parseval identity, coherence bound, selected-block conditioning, and source-scale violation.

B.1 The selected columns

We build column vectors $A = (a_1 \ \cdots \ a_n) \in \mathbb{R}^{k \times n}$, and then define $Q = A^T$.

Fix $H_* > 1$, $B > 0$, $e \geq 0$, and $K \geq 1$. Choose $\eta > 0$ so small that

$$e^{2\eta} < H_*.$$

Choose m large and set

$$k = m + 1, \quad \epsilon = e^{-\eta/k}, \quad s = (1 - \epsilon^2)^{1/2}, \quad \alpha = \frac{1}{k}.$$

All smallness requirements below are met by taking k sufficiently large. Define the diagonal scales

$$d_t = \alpha \epsilon^{t-1}, \quad 1 \leq t \leq m.$$

The first $k = m + 1$ column labels are the intended QRCP labels:

$$I_{\text{piv}} = (1, 2, \dots, m, m + 1).$$

Choose signs $\sigma_t \in \{\pm 1\}$ and set $\beta = \frac{1}{2}$. This constant controls the strictly upper-triangular couplings among the first m selected columns. Define $R_\beta \in \mathbb{R}^{m \times m}$ by

$$(R_\beta)_{t,q} = \begin{cases} d_t, & q = t, \\ -\beta \sigma_t \sigma_q s d_t, & t < q, \\ 0, & t > q. \end{cases}$$

The first m selected columns are

$$a_q = \begin{pmatrix} (R_\beta)_{:,q} \\ 0 \end{pmatrix}, \quad 1 \leq q \leq m.$$

In matrix form their first m coordinates are

$$R_\beta = \begin{pmatrix} d_1 & -\beta \sigma_1 \sigma_2 s d_1 & \cdots & -\beta \sigma_1 \sigma_m s d_1 \\ 0 & d_2 & \cdots & -\beta \sigma_2 \sigma_m s d_2 \\ \vdots & \vdots & \ddots & \vdots \\ 0 & 0 & \cdots & d_m \end{pmatrix}.$$

We now define the final selected column. Set

$$\gamma_0 = \frac{1}{4}, \quad \tau_0 = \frac{1}{16}.$$

The first number controls the size of the first-block component of the final selected column; the second fixes its final residual scale. Define

$$r = \tau_0 d_m^2, \quad \eta_p = \tau_0^{1/2} d_m,$$

so that $\eta_p^2 = r$. After the first m selected columns have been chosen, their span is $\mathbb{R}^m \oplus \{0\}$; projecting the final selected column away from this span removes its first-block part and leaves only η_p . Thus its squared residual at that moment is r .

Define $z \in \mathbb{R}^m$ by

$$z_t = \begin{cases} \gamma_0 \sigma_t s d_t, & 1 \leq t < m, \\ \gamma_0 \sigma_m (1 - \tau_0)^{1/2} d_m, & t = m. \end{cases}$$

The final selected column is

$$a_{m+1} = \begin{pmatrix} z \\ \eta_p \end{pmatrix},$$

Thus the selected block of A is

$$R_+ = \begin{pmatrix} R_\beta & z \\ 0 & \eta_p \end{pmatrix}.$$

Equivalently,

$$R_+ = \begin{pmatrix} d_1 & -\beta \sigma_1 \sigma_2 s d_1 & \cdots & -\beta \sigma_1 \sigma_m s d_1 & \gamma_0 \sigma_1 s d_1 \\ 0 & d_2 & \cdots & -\beta \sigma_2 \sigma_m s d_2 & \gamma_0 \sigma_2 s d_2 \\ \vdots & \vdots & \ddots & \vdots & \vdots \\ 0 & 0 & \cdots & d_m & \gamma_0 \sigma_m (1 - \tau_0)^{1/2} d_m \\ 0 & 0 & \cdots & 0 & \tau_0^{1/2} d_m \end{pmatrix}.$$

Since $Q = A^T$, the selected row matrix $M(Q)$ is R_+^T up to the fixed ordering.

B.2 The full matrix and the identity completion

We now display the whole matrix. The construction has four column blocks:

$$A = (R_+ \quad X \quad F \quad G) \in \mathbb{R}^{k \times n}, \quad k = m + 1.$$

We use the splitting

$$\mathbb{R}^k = \mathbb{R}^m \oplus \mathbb{R}, \quad I_k = \begin{pmatrix} I_m & 0 \\ 0 & 1 \end{pmatrix}.$$

This block split separates the two residual mechanisms in the construction. The first m coordinates carry the QRCP chain and the triangular amplification; the last coordinate stores the residual mass that remains after the chain has been selected. Thus, $AA^T = I_k$ is proved by checking the off-diagonal blocks, the upper-left block, and the lower-right scalar separately.

The cross block X

The final selected column $\begin{pmatrix} z \\ \eta_p \end{pmatrix}$ creates an off-diagonal block $z\eta_p$. We cancel it by adding two columns.

Choose

$$\theta_1 = \frac{3}{5}, \quad \theta_2 = \frac{4}{5}, \quad b_1 = \frac{7}{15}, \quad b_2 = \frac{9}{10}, \quad \theta_1 b_1 + \theta_2 b_2 = 1.$$

Define

$$X = \begin{pmatrix} \theta_1 z & \theta_2 z \\ -b_1 \eta_p & -b_2 \eta_p \end{pmatrix}.$$

Then

$$R_+ R_+^T = \begin{pmatrix} R_\beta R_\beta^T + z z^T & z \eta_p \\ \eta_p z^T & \eta_p^2 \end{pmatrix}$$

and

$$X X^T = \begin{pmatrix} (\theta_1^2 + \theta_2^2) z z^T & -z \eta_p \\ -\eta_p z^T & (b_1^2 + b_2^2) \eta_p^2 \end{pmatrix}.$$

So the off-diagonal blocks in $R_+ R_+^T + X X^T$ are zero. Put

$$\kappa_z = 1 + \theta_1^2 + \theta_2^2, \quad \kappa_\eta = 1 + b_1^2 + b_2^2.$$

The pure frame completion block F

After R_+ and X have been placed, the upper-left block still missing from I_m is

$$M_{\text{rem}} = I_m - R_\beta R_\beta^T - \kappa_z z z^T.$$

For m sufficiently large, M_{rem} is positive definite.

Decompose this missing upper-left block into small rank-one atoms:

$$M_{\text{rem}} = \sum_{h=1}^{N_{\text{frame}}} W_h u_h u_h^T, \quad 0 < W_h < d_m^2, \quad \|u_h\|_2 = 1.$$

The atom bound is deliberately at the same scale as the smallest selected-chain residual. It ensures that no frame column can overtake an intended QRCP pivot. Such a decomposition is obtained by taking a spectral decomposition of M_{rem} and subdividing each eigenvalue into sufficiently many positive pieces. The number of atoms satisfies

$$N_{\text{frame}} \leq \frac{\text{Tr}(M_{\text{rem}})}{d_m^2} + 2m \leq \frac{m}{d_m^2} + 2m.$$

For each atom add one column supported only in the first m coordinates:

$$f_h = \begin{pmatrix} \sqrt{W_h} u_h \\ 0 \end{pmatrix} \in \mathbb{R}^m \oplus \mathbb{R}, \quad 1 \leq h \leq N_{\text{frame}}.$$

Equivalently, the whole frame block is the explicit matrix

$$F = \begin{pmatrix} \sqrt{W_1} u_1 & \sqrt{W_2} u_2 & \cdots & \sqrt{W_{N_{\text{frame}}}} u_{N_{\text{frame}}} \\ 0 & 0 & \cdots & 0 \end{pmatrix} \in \mathbb{R}^{k \times N_{\text{frame}}}.$$

Then

$$FF^T = \begin{pmatrix} \sum_{h=1}^{N_{\text{frame}}} W_h u_h u_h^T & 0 \\ 0 & 0 \end{pmatrix} = \begin{pmatrix} M_{\text{rem}} & 0 \\ 0 & 0 \end{pmatrix}.$$

Thus F completes exactly the missing upper-left block, produces no off-diagonal block, and contributes no mass to the last coordinate.

The same small-atom bound controls QRCP residuals. At a selected prefix S_ℓ with $\ell < m$, the residual score of f_h is at most its full squared norm:

$$\|f_h\|_2^2 = W_h < d_m^2 \leq d_{\ell+1}^2.$$

At the last prefix S_m , the selected span is $\mathbb{R}^m \oplus \{0\}$, so f_h has residual score zero. Hence the pure frame columns never compete with the prescribed pivots.

The residual-only block G

After the blocks R_+ , X , and F have been placed, the upper-left block has already become I_m and the off-diagonal block is zero. Since F has no last-coordinate component, the only lower-right contribution so far is the selected-and-cross contribution $\kappa_\eta r$. The amount still missing is therefore

$$\mu_{\text{res}} = 1 - \kappa_\eta r.$$

For m sufficiently large, $r = \tau_0 d_m^2$ is small and $\mu_{\text{res}} > 0$.

Split the remaining scalar into small pieces

$$\mu_{\text{res}} = e_1 + \cdots + e_{N_{\text{res}}}, \quad 0 < e_j < \frac{r}{2},$$

choosing the e_j also to avoid the finitely many residual equalities if a fixed tie-breaking convention is desired. This can be done with

$$N_{\text{res}} \leq \frac{2}{r} + 2.$$

For each piece add one column supported only in the last coordinate:

$$g_j = \begin{pmatrix} 0 \\ \sqrt{e_j} \end{pmatrix} \in \mathbb{R}^m \oplus \mathbb{R}, \quad 1 \leq j \leq N_{\text{res}}.$$

Equivalently,

$$G = \begin{pmatrix} 0_{m \times N_{\text{res}}} \\ \sqrt{e_1} \sqrt{e_2} \cdots \sqrt{e_{N_{\text{res}}}} \end{pmatrix} \in \mathbb{R}^{k \times N_{\text{res}}}.$$

Therefore

$$GG^T = \begin{pmatrix} 0_{m \times m} & 0 \\ 0 & \mu_{\text{res}} \end{pmatrix}.$$

These columns cannot compete with the final selected column after the first m pivots, because each has squared residual $e_j < r/2 < r$.

Putting the four blocks together,

$$AA^T = R_+R_+^T + XX^T + FF^T + GG^T.$$

The upper-left block is

$$R_\beta R_\beta^T + \kappa_z z z^T + M_{\text{rem}} = I_m,$$

the off-diagonal block is zero, and the lower-right scalar is

$$\kappa_\eta r + \mu_{\text{res}} = 1.$$

Hence

$$AA^T = \begin{pmatrix} I_m & 0 \\ 0 & 1 \end{pmatrix} = I_k.$$

B.3 Main lemmas

This section isolates the estimates used to prove the main theorem.

Lemma 21 (Pivot order). *QRCP applied to $A = Q^T$ selects*

$$I_{\text{piv}} = (1, 2, \dots, m, m+1).$$

Proof. Define $R_j(S) = \|(I_k - P_S)a_j\|_2^2$, where P_S is the orthogonal projector onto $\text{span}\{a_i : i \in S\}$. For $0 \leq \ell \leq m$, put $S_\ell = \{1, \dots, \ell\}$. At prefix S_ℓ with $0 \leq \ell < m$, the intended next label is $\ell + 1$ and

$$R_{\ell+1}(S_\ell) = d_{\ell+1}^2.$$

For a later selected-chain label q with $\ell + 1 < q \leq m$, the upper-triangular form of R_β gives

$$R_q(S_\ell) = \beta^2 s^2 \sum_{a=\ell+1}^{q-1} d_a^2 + d_q^2.$$

Using $d_a = \alpha \epsilon^{a-1}$ and $s^2 = 1 - \epsilon^2$, this becomes

$$R_q(S_\ell) = d_{\ell+1}^2 \left(\beta^2 + (1 - \beta^2) \epsilon^{2(q-\ell-1)} \right) < d_{\ell+1}^2,$$

because $0 < \epsilon < 1$ and $0 < \beta < 1$.

The final selected label $m+1$ satisfies, for $0 \leq \ell < m$,

$$R_{m+1}(S_\ell) = \gamma_0^2 (d_{\ell+1}^2 - r) + r.$$

Since $r = \tau_0 d_m^2 \leq \tau_0 d_{\ell+1}^2$,

$$R_{m+1}(S_\ell) \leq (\gamma_0^2 + \tau_0) d_{\ell+1}^2 = \frac{1}{8} d_{\ell+1}^2 < d_{\ell+1}^2.$$

The columns in X , F , and G are all smaller. The two columns in X have the same form as the final selected column, but with both coefficients strictly smaller than one; the constants above give residual scores strictly below the final selected column at every prefix. For a pure frame column f_h , the atom bound gives, for $\ell < m$,

$$\|f_h\|_2^2 = W_h < d_m^2 \leq d_{\ell+1}^2.$$

For a residual-only column g_j , its residual score is at most $e_j < r/2 < d_{\ell+1}^2$.

At S_m , the final selected label has residual score

$$R_{m+1}(S_m) = r,$$

whereas the columns in X have last-coordinate residual $b_i^2 r < r$, each frame column has residual zero, and each residual-only column has residual $e_j < r/2 < r$. Thus $m+1$ is selected at the last step. \square

Lemma 22 (Parseval identity). *The constructed matrix satisfies*

$$AA^T = I_k, \quad \text{and hence} \quad Q^T Q = I_k.$$

Proof. Using the block notation from the construction,

$$A = \begin{pmatrix} R_+ & X & F & G \end{pmatrix}.$$

Thus

$$AA^T = R_+ R_+^T + X X^T + F F^T + G G^T.$$

The selected block contributes

$$R_+ R_+^T = \begin{pmatrix} R_\beta R_\beta^T + z z^T & z \eta_p \\ \eta_p z^T & \eta_p^2 \end{pmatrix}.$$

The cross block X cancels the off-diagonal entries because $\theta_1 b_1 + \theta_2 b_2 = 1$. The pure frame block F contributes exactly M_{rem} in the upper-left corner and contributes zero to both the off-diagonal blocks and the lower-right entry. The block G contributes exactly the remaining lower-right scalar

$$\mu_{\text{res}} = 1 - \kappa_{\eta^T}.$$

Therefore

$$AA^T = \begin{pmatrix} I_m & 0 \\ 0 & 1 \end{pmatrix} = I_k.$$

□

Lemma 23 (Coherence bound). *For m sufficiently large, the constructed matrix satisfies*

$$\mu(Q) < H_*.$$

Proof. Because $Q = A^T$, the squared norm of a row of Q is the squared norm of the corresponding column of A . We first prove the row-leverage bound

$$\max_i \|Q(i, \cdot)\|_2^2 = \alpha^2.$$

For the first m selected columns, direct summation gives

$$\|a_q\|_2^2 = d_q^2 + \beta^2 s^2 \sum_{t=1}^{q-1} d_t^2 = \alpha^2 \left(\beta^2 + (1 - \beta^2) \epsilon^{2(q-1)} \right) \leq \alpha^2,$$

with equality at $q = 1$. For the final selected column,

$$\|(z^T, \eta_p)\|_2^2 = \|z\|_2^2 + \eta_p^2 = \gamma_0^2 (\alpha^2 - r) + r < \alpha^2,$$

because $0 < \gamma_0 < 1$ and $r < \alpha^2$.

For the two columns in X ,

$$\|(\theta_i z^T, -b_i \eta_p)\|_2^2 = \theta_i^2 \|z\|_2^2 + b_i^2 \eta_p^2 < \|z\|_2^2 + \eta_p^2 < \alpha^2,$$

since $0 < \theta_i, b_i < 1$.

For a pure frame column in F ,

$$\|f_h\|_2^2 = W_h < d_m^2 \leq d_1^2 = \alpha^2.$$

Finally, a residual-only column in G has squared norm

$$e_j < r/2 < \alpha^2.$$

Thus the maximum row leverage is α^2 .

Therefore

$$\mu(Q) = \frac{n}{k} \alpha^2 = \frac{n}{k^3}.$$

Using the count

$$n = m + 3 + N_{\text{frame}} + N_{\text{res}},$$

together with

$$N_{\text{frame}} \leq \frac{m}{d_m^2} + 2m, \quad N_{\text{res}} \leq \frac{2}{\tau_0 d_m^2} + 2,$$

we estimate the two filler contributions separately. Since

$$d_m^2 = \alpha^2 \epsilon^{2m-2} = \frac{1}{k^2} \exp\left(-\frac{2\eta(m-1)}{k}\right),$$

we have

$$\frac{m}{k^3 d_m^2} = \frac{k-1}{k} \exp\left(\frac{2\eta(k-2)}{k}\right) \rightarrow e^{2\eta}.$$

The remaining terms contribute only $O(k^{-1})$ after division by k^3 . Hence

$$\mu(Q) \leq e^{2\eta} + o(1).$$

Because $e^{2\eta} < H_*$, taking k sufficiently large gives $\mu(Q) < H_*$. □

Lemma 24 (Selected-block pressure). *Let*

$$Z = \|R_\beta^{-1} z\|_2^2.$$

Then $M(Q)$ is nonsingular and

$$\gamma(Q, I_{\text{piv}})^2 \geq \frac{1+Z}{r} \geq \frac{Z}{r}.$$

Moreover, Z eventually dominates every fixed polynomial in k .

Proof. The matrix R_+ is upper triangular with positive diagonal entries d_1, \dots, d_m, η_p , so it is nonsingular.

Let $x = R_\beta^{-1} z$ and set

$$v = \begin{pmatrix} -x \\ 1 \end{pmatrix}.$$

Then

$$R_+ v = \begin{pmatrix} 0 \\ \eta_p \end{pmatrix}, \quad \|v\|_2^2 = 1 + Z.$$

Thus

$$\sigma_{\min}(R_+)^2 \leq \frac{\eta_p^2}{1+Z} = \frac{r}{1+Z},$$

which gives the inverse-norm lower bound.

It remains to see why Z is large. Write $x_t = \sigma_t y_t$. Back-substitution gives

$$y_m = \gamma_0 (1 - \tau_0)^{1/2}, \quad y_t = s \left(\gamma_0 + \beta \sum_{q=t+1}^m y_q \right), \quad t < m.$$

Hence

$$y_t = \gamma_0 s (1 + \beta s)^{m-t-1} \left(1 + \beta (1 - \tau_0)^{1/2} \right),$$

and consequently

$$Z \geq \gamma_0^2 s^2 (1 + \beta s)^{2(m-2)}.$$

Since $m = k - 1$ and there are constants $0 < c < C < \infty$ such that

$$ck^{-1/2} \leq s \leq Ck^{-1/2},$$

this lower bound grows faster than any fixed power of k . □

Lemma 25 (Source-scale denominator). *The row count satisfies*

$$r(n - k + 1) \leq C_{\text{den}} k, \quad C_{\text{den}} = 3.$$

Proof. Since $k = m + 1$ and $n = m + 3 + N_{\text{frame}} + N_{\text{res}}$,

$$n - k + 1 = 3 + N_{\text{frame}} + N_{\text{res}}.$$

The frame part gives

$$rN_{\text{frame}} \leq \tau_0 d_m^2 \left(\frac{m}{d_m^2} + 2m \right) = \tau_0 m + 2\tau_0 d_m^2 m.$$

The residual-only part gives

$$rN_{\text{res}} \leq 2 + 2r.$$

Therefore

$$r(n - k + 1) \leq 3r + \tau_0 m + 2\tau_0 d_m^2 m + 2 + 2r.$$

Because $d_m^2 = O(k^{-2})$ and $r = \tau_0 d_m^2$, the finite remainder $5r + 2\tau_0 d_m^2 m < 1$ for k large. Hence

$$r(n - k + 1) \leq 3 + \tau_0 m \leq 3k$$

for all sufficiently large k . □

B.4 Proof of the obstruction theorem

We now assemble the preceding lemmas.

Proof of Theorem 2. Choose $k = m + 1 \geq K$ large enough so that the following hold:

- (i) the coherence estimate in Lemma 23 gives $\mu(Q) < H_*$;
- (ii) the denominator estimate in Lemma 25 holds;
- (iii) the triangular growth satisfies

$$Z > C_{\text{den}} B^2 k^{2e+2}.$$

The last condition is possible by Lemma 24, since Z dominates every fixed polynomial in k .

By Lemma 22, the matrix $Q = A^T$ has orthonormal columns. By Lemma 21, exact QRCP selects

$$I_{\text{piv}} = (1, 2, \dots, m, m + 1).$$

By Lemma 24, $M(Q)$ is nonsingular and

$$\gamma(Q, I_{\text{piv}})^2 \geq \frac{Z}{r}.$$

Therefore

$$\frac{\gamma(Q, I_{\text{piv}})^2}{k(n - k + 1)} \geq \frac{Z}{rk(n - k + 1)}.$$

Using Lemma 25,

$$r(n - k + 1) \leq C_{\text{den}} k,$$

we obtain

$$\frac{\gamma(Q, I_{\text{piv}})^2}{k(n-k+1)} \geq \frac{Z}{C_{\text{den}}k^2} > B^2k^{2e}.$$

Taking square roots gives

$$\frac{\gamma(Q, I_{\text{piv}})}{\sqrt{k(n-k+1)}} > Bk^e.$$

This proves the theorem. □